공학박사 학위논문

정적 연소실 내 직류 전기장 인가가 연소 특성의 변화에 미치는 영향

Effects of DC Electric Field on Flame Propagation Characteristics in a Constant Volume Chamber

2017 년 2 월

서울대학교 대학원

기계항공공학부

손 경 민

Abstract

Effects of DC Electric Field on Flame Propagation Characteristics in a Constant Volume Chamber

Kyugmin Shon

Department of Mechanical and Aerospace Engineering

The Graduate School

Seoul National University

In modern times, fossil fuels are used for over 80% of energy consumption in human society. Therefore, developing more efficient and clean combustion systems is an important priority. One of the interesting topics in the combustion research field is the electrically assisted system. It has the advantage of changing combustion characteristics with relatively little energy consumption, and furthermore, control of high voltages becomes relatively easy, as the technology of semiconductor devices develops. Nonetheless, despite extensive previous research, the detailed interpretation of the effects is limited. Especially, the effects of timing and duration of applied electric field on the growth of flame has seldom been reported.

Thus, the goal of this dissertation is to investigate the effect of timing of electric field excitation on the propagation speed in a constant volume chamber. To establish the influence on the growth of flame, a cylindrical constant volume chamber in which the directions of the electric field and the flame propagation are parallel to each other is introduced. Moreover, a control and monitoring system to minimize the deviation is developed.

The three distinct regimes are identified depending on the polarity and timing of the electric field excitation. Regime I is defined as an effective regime under the condition of the positive potential. When a positive potential is applied, the enhancements of combustion characteristics are observed only within the initial stage of flame kernel growth; the improvement on other periods of combustion is negligible. From this phenomenon, it is elucidated that that the free electrons in the flame front trigger the increment of chemical reaction. The effects of the polarity of excitation voltage and the equivalence ratio of the mixture are investigated in regime I. The effect of the electric field is more pronounced at the positive potential and lean condition in this regime. Regimes II and III are classified by the current flow when a negative potential is applied. Regime II shows a slight increment of the current and it is saturated in hundreds of μA when 20% of mass burn. In this regime, the effect per unit time is less effective than that of regime I. Nonetheless, the total effect is better than that for regime I, as the effective duration is relatively longer. Regime III appears just after regime II, and it shows a sharp increase in current flow. The dramatic rise of peak pressure and advance of its timing are observed near the last period of combustion. This result is confirmed as an extra combustion of unburned

gas near the wall of the chamber.

In addition to the ionic wind effect which is considered as a major mechanism of the DC electric field, the results of the experiments confirm that the chemical reaction rate and the extra combustion of unburned gas near the wall are able to play an important role. The results presented in this dissertation show a possibility of the electric field excitation for application of the reciprocating engines. Considering that the experimental condition of this study is fixed in premixed air-fuel mixture, it is likely to applicable to engines with low viscosity fuels such as CNG. Further studies will be required to applying the electric field assisted combustion systems to the real engines in the future.

Keywords **: Electric field, Flame propagation speed, Ionic wind, Premixed flame, Constant Volume Chamber**

Student Number **: 2006-20938**

TABLE OF CONTENTS

LIST OF FIGURES

LIST OF TABLES

LIST OF SYMBOLS

C_p	specific heat at constant pressure, J/mol·K
C_v	specific heat at constant volume, J/mol·K
γ	specific heat ratio
E	electric field intensity, V/m
Q	heat transfer, J
t	time, ms
t_s	start time of high voltage excitation, ms
t_e	end time of high voltage excitation, ms
t_{10}	10% burn time
t_{85}	85% burn time
t_{Pmax}	maximum pressure time, ms
T	temperature, K
P	pressure, bar
P_{max}	maximum pressure, bar
U	internal energy, J
V	volume of chamber, mm^3

V_e amplitude of DC high voltage excitation, kV

V_{th} threshold voltage, kV

I current, mA

x_b burned mass fraction, %

ϕ fuel/air equivalence ratio

Acronym

SOI start of ignition

DC direct current

AC alternating current

HF high frequency

RSD relative standard deviation

Chapter 1. Introduction

1.1 Motivation

Combustion is one of the strongest and efficient power sources in human society. Since human beings became aware of how to control fire, combustion has been fundamental to our existence. As it can generate energy from a simple process, it is used for many activities like cooking, warming, and so on. In modern days, the usage of combustion systems occupies over 80% of energy consumption in human society and is spread to many systems including transporting, industrial processing, electricity generation, etc.

However, Combustion is deeply relevant to critical issues, such as energy crisis, global warming, environmental pollution, and so on. Combustion process generates air pollutants including carbon dioxide (CO2) and nitrogen oxides (NOx), sulfur oxides (Sox), and soot. These pollutants have caused negative effects such as the greenhouse effect, acid rain, etc. Furthermore, the amount of fossil fuel is limited and a shortage of the fuel causes the increase of the prices. Consequently, it is highly required to develop ever more powerful, efficient, and clean combustion systems.

A wide range of challenges of technologies to enhance the combustion process have been conducted. For example, there have been combustion systems that can operate under the conditions of leaner air-fuel ratio to reduce the emissions, and those

of higher pressure to improve the efficiency [1]. However, traditional combustion technologies under these severe conditions face problems such as flammability, ignitibility, and stability. Those challenges require new methods to overcome the limitations. One of the simple and easy ways to enhance the combustion is elevating the temperature to accelerate the air-fuel reaction rate [2]. However, this method requires a large amount of energy to control the reaction speed; therefore, it is uneconomical. Other ways to enhance the reaction rate without elevation of temperature are adding additives (more reactive chemicals)or reforming fuels [2]. These methods also have problems: they require additional complex pre-combustion systems to control, and it is hard to control them in-situ and real time.

Another way and one of the interesting topics in the combustion research field is electrically assisted combustion. The main idea of this method is based on the fact that the flame contains plasma—molecules are thermally dissociated into charged particles including free electrons and ions—and it can be influenced by an external electrical energy source. Control of electrical energy (i.e., high voltage) has become relatively easy as the technology of semiconductor devices has developed.

Even more than 200 years ago, scientists observed that charged species in the flame front were affected by the electric field outside of the flame. Brande [3] performed an experiment placing a small flame between two charged electrodes. Brande reported that the flame front is attracted toward one of the electrodes when an electric potential is applied. Depending on the substances of gasses, the flame front bends toward either the positive electrode or the negative one; as a consequence, one of the electrodes gains more heat than the other one. These results evidently show that

different charged particles are attracted toward the different poles of the electrode. This study is one of the first inklings of the interaction between flame and electric field, and implies that heat and mass transfer in combustion can be controlled by the external electric field. From then on, many researchers inspired by this observation have established theories to enhance the combustion characteristics and explain the mechanism.

1.2 Literature Review

For decades, the effects of electric field on flame propagation have been extensively studied. Since the report of Jaggers et al. [4] that the flame speed is enhanced by the electric field in natural gas (i.e., methane), a number of experiments have been conducted on hydrocarbon fuels. Methane is one of the most frequently studied materials in combustion for two reasons. First, it has the simplest molecular structure among hydrocarbon fuels and its combustion mechanisms are well known (e.g., GRI-Mech). Second, methane is a relatively abundant and attractive fuel, as it is the main component of natural gas. Researchers have found that many types of flames, such as premixed Bunsen flame [5]–[8], counterflow flame [9]–[11], premixed spherical flame [12]–[14], nonpremixed jet flame [15], [16] using DC [13], [17], [18] or AC [6], [19], electric fields are known to cause the improvements of combustion characteristics including flame speed [20]–[22], flammability limit [23], soot emission [24], and flame stabilization [7], [11], [18]. The possible mechanisms to

explain the phenomenon are ionic wind effect, kinetic effect, and conversion of electrical energy into heat. Several important previous studies on electric field-assisted combustion for enhancing the propagation speed are described below.

Chattock [25] investigated the electric wind effect on the needle-plate and the needle-ring geometry electrode. This report experimentally and quantitatively shows the relationship between the electrical current and the pressure (i.e., hydrodynamical flow). When the high voltage is charged at the electrode, a corona discharge occurs, and charged ions are generated around the electrode. These charged ions are attracted along with the direction of electric field; and as a result, a bulk flow of charged particles occurs

Yonggang et al. [26] investigated the effect of ionic wind on the heat transfer rate from a heated vertical copper plate. They conducted the experiments using different types of discharge including corona discharge, dielectric barrier discharge, and glow discharge. As a consequent, they reported that the heat transfer coefficient increases by several times compared to the natural convection condition (i.e., without an electrical assistant).

Go et al. [26] demonstrated the forced convection heat transfer using an ionic wind. They constructed a flat plate exposed to a bulk flow and generated a corona discharge to cause an ionic wind. This study reports that an increment of heat transfer coefficients is not due to the induced electrical thermal effects, but due to the bulk flow of ions.

Lewis [20] investigated the effects of the electric field on the industrial Bunsen

burner. They examined many types of hydrocarbon flame from methane to butane, and found that the hydrocarbon flame is always attracted to the negative electrode. From this result, they concluded that the positive ions play a bigger role than negative ions in the ionic wind effect.

Calcote et al. [5] observed that flame stability is influenced by the longitudinal electric fields on the Bunsen flame. They reported that the burning velocity and the flame stabilization are increased or decreased depending on the direction and the strength of electric field. From the experimental results, the momentum transfer from positive ions to the gas is suggested, which matches with the conclusion of Lewis [20]. This enhancement was named as "the ionic wind effect", and it is considered as one of the major mechanism of the DC electric field on flame combustion.

The burning velocity of methane and ethylene gas in the vertical tube was measured by Jaggers et al. [4]. They observed enhancement of flame propagation when DC, AC, and HF electric fields are excited across the flame. Particularly in the case of HF excitation, they concluded that electrons are first agents because the momentum transfer from heavy ions is negligible at relatively high frequency. The energy of the chemical reaction is greater than the electrical input; this is not accounted for by the temperature rise of the gas mixture, but by that of electrons. These observations imply that the change of electron temperature influences reaction rate.

By changing the polarity of applied DC electric field on Bunsen burner, Marcum et al. [21] concluded that the negatively charged species do not play a major role in the enhancement of flame propagation. Additionally, they demonstrated that time

delay is required to complete the change of flame front—the collision response time to development of the ionic wind effect [9]. Under the same condition, Wisman et al. [18] observed flame wrinkling and proposed thermo-diffusive instability by the production of radicals through dissociative recombination.

Won et al. [22], [27] investigated the propagation speed in tribrachial flames with applied AC and DC electric fields. As the effect of DC electric field, polarity effect—enhancement is maximized with the positive DC field (i.e., positive ions are attracted toward the unburned zone) rather than negative DC field. They also reported that the reattachment velocity increased with respect to the AC electric field. In both cases of DC and AC electric field, they concluded that the propagation speed is influenced by the electric field intensity.

Boom et al. [17] reported that the chemical reaction induced by the electric field causes an increase in adiabatic burning velocity. They suggested numerical modeling indicating that the excitation of nitrogen molecules is the main mechanism.

Affections of AC electric field on premixed Bunsen flame were studied by Kim et al. [6], [7], [11]. Under a wide range of applied voltages and frequencies, apparent different regimes are classified. Particularly, by observing the stabilization of flames, the transition frequency regimes near the 50Hz were reported. They suggested simple modelling about the kinetic collision of ions[9] and elucidated that a delay time to develop the ionic wind is required.

Duan et al. [14] investigated the effects of negative DC electric field intensity and distribution on spherical flame in a constant volume chamber. By measuring the

stretch rate and the laminar velocity, they confirmed that the promotion of flame propagation is closely related to the electric field unity factors.

It has also known shown that the electric field influences the soot particle formation. Bowser et al. [28] found that soot emission can be controlled electrically. The application of an electric field reduces the size of the soot particles and the total amount of the emissions. They explained that the charged soot particles are rapidly separated from the soot formation zone.

Saito et al. [24] investigated the variations of flame shape and soot emission by applying the electric field. They showed that the soot emission can be suppressed by the electric field. This phenomenon is explained by the increase of the flame temperature which is caused by the improved mixing of fuel and surrounding gas.

Cha et al. [15] showed that the dielectric barrier discharge reduces the soot formation in the diffusion coflow jet burner. As the applied voltage to the dielectric barrier discharge reactor increases, the flame length and the soot luminosity decreases. They elucidated that the ionic wind effect increases the radial convection, and the balance between the convection and the diffusion results in the change flame length.

Various studies have proposed mechanisms of the interaction between the flame propagation and the electric field; however, the detailed interpretation of the effects is not clear yet. This is because the combustion itself is coupled with the chemical, thermal, and hydrodynamic effects and is a very complex phenomenon. For example, in the case of transient flame in a constant volume chamber, the shape of the electrode (i.e., distribution of electric field) is known to an important factor [14]. Additionally,

improvement of combustion is not equally occurring in the whole combustion period, but is concentrated in the initial period of combustion [23], [29]. These results demonstrate that the timing and duration of applied electric field are important, but this subject has been little elucidated in the literature.

1.3 Objectives of Present Study

The goal of this dissertation is to investigate the effects of the electric field on the propagation speed in a constant volume chamber by varying timings and amplitudes of the high voltage excitation. To establish the influence of the electric field on the growth of flame, the cylindrical constant volume chamber—in which the directions of combustion and electric field are aligned parallel—is designed, and the experiments are performed in it.

In Chapter 2, the design of the experimental system is introduced. Firstly, the schematic shape of the constant volume chamber is presented, and its characteristics are discussed. Secondly, the experimental system for varying the timing of the electric field is specified. The system is composed of five sub-parts—the constant volume chamber, the data acquisition and control system, the high voltage excitation system, the gas exchange system, and an ignition system. Subsequently, the analysis method is explained.

Chapter 3 discusses the results by varying the timing of the positive potential. When a positive potential is applied to the high voltage inside the chamber, the

vectors of the electric field and the flame propagation are aligned in the opposite direction to each other.

In Chapter 4, the effects of the negative potential are observed. Obviously, the two vectors are aligned in the same direction. In this case, the positive particles in the flame front are attracted to the unburned zone, and the influence of the ionic wind effect is predominant.

In Chapter 5, the effective regimes are classified by timing and polarity of the electric field. As described in previous chapters, the results demonstrate that there are three different regimes—each regime has noticeable characteristics depending on the current flow and the pressure history. The combustion characteristics are discussed in detail, and the results are compared with those in other studies.

Finally, the conclusions are summarized in Chapter 6.

Chapter 2. Experimental Methods and Procedure

2.1 Experimental Apparatus

The structure of the combustion chamber is shown in Figure 2.2. A cylindrical constant volume chamber with a diameter of 88 mm and height of 10 mm was adopted. As the diameter of the combustion chamber is greater than the height, the combustion process is assumed as a radially propagating laminar flame, and axial direction is thus neglected. In Figure 2.1 (a), the exploded view of the chamber shows that the chamber is made up of three layers. The top and the bottom layers are made of acetal resin, and function as an electrical insulator for high voltage excitation. A spark plug for the central ignition flame is placed in the center of the top layer; a piezoelectric pressure transducer (Kistler, 6051A) to measure pressure history was placed in the center of the bottom layer. The middle layer, the sidewall of the cylinder, is made of aluminum and functions as a high voltage electrode, connected to the high voltage excitation system. The other terminal of the high voltage excitation system—the ground of high voltage system—is connected to the body of the spark plug and the piezoelectric transducer. Consequently, the structure of the combustion chamber is similar to that of the coaxial capacitor. Figure 2.4 shows the simulation result of DC electric field inside the chamber. The distribution of the electric field is axisymmetric and aligned well with the direction of the flame propagation.

Figure 2.3 shows the experimental system. The system consists of five subparts: the constant volume chamber, a high voltage excitation system, a gas exchange system, an ignition system, and a DAQ/control system.

The high voltage excitation system is made up of the high voltage amplifier (Trek, 10/10B-FG) and auxiliary circuit to measure current and voltage. The preset signal generated from the DAQ/control system is amplified by the high voltage excitation system and applied to the high voltage electrode, the sidewall of the constant volume chamber.

The gas exchange system consists of multiple valves, a premix chamber, and a vacuum pump; it is controlled automatically by the DAQ/control system to exhaust burned gas and intake unburned mixture in the combustion chamber. The valves (shown in Figure 2.2) are controlled by servo motors. The premix chamber is used to ensure consistent air/fuel mixture. Before the experiment, chemically pure grade CH_4 (99.999%) and O_2/N_2 mixture gas (21% O_2 and 79% N_2 by volume) was supplied to the premix chamber at the corresponding partial pressure, and maintained until complete mixing was guaranteed.

The ignition system is composed of the spark plug, an inductive ignition coil, and an auxiliary control circuit. The ignition coil is charged by control circuit and the dwell time is set to 4ms. When the current is cut off by the control system, the arc discharge occurs on the spark plug, which we define as the start of ignition (SOI) and set as the origin of timing to synchronize the whole system.

The DAQ/control system is made up of a microprocessor (ATSAMX8E, Atmel)

and data acquisition device (National Instruments, NI USB-6363). The DAQ/control system handles the whole system—the signal generation, the data measurement and its record, and the control. As shown in the timing chart, Figure 2.6, the signals and timings including DAQ control signal, ignition signal, high voltage profile, and measured data are synchronized with respect to the SOI.

To minimize the deviation of experiments and guarantee repeatability, the monitoring software was developed based on LabVIEW and Python 2 (Figure 2.5). This software controls the entire experimental setup, saves the measured data, and monitors the states of the system in real-time. The experimental procedure can be summarized as follows. The first step is evacuating the constant volume combustion chamber with the gas exchange system. Second, the premixture gas of air and fuel is charged into the chamber in compliance with the initial condition of the experiment until the quiescent state is guaranteed. Third, the high voltage is applied to the electrode with respect to the prepared voltage profile; simultaneously, the combustion process is initiated by the ignition system. Before the main experiment and measurement, dummy procedure was carried out 100 times to stabilize the system and confirm ambient temperature. After the entire system entered the steady state, the experiments were repeated at least eight times for each condition.

2.2 Analysis of Experimental Result

The shot-by-shot result of the repeated experiment in baseline (i.e., without electric field) is shown in Figure 2.7. The solid line presents the average curve. To quantify the repeatability and deviation of results, the relative standard deviation (%RSD) is calculated. The calculated %RSD of maximum pressure and its time are 0.50% and 1.54% respectively, indicating good repeatability.

The actual results of the experiment are depicted in Figure 2.8, where the DC +7kV is excited from SOI and has a duration of 4 ms. As shown in the measured voltage curve, rise time and falling time are smaller than 0.2 ms. The pressure history is nearly flat in the early stage of combustion, within 3 ms after SOI. Subsequently, the pressure rapidly rises for ~20 ms. It finally reaches the maximum pressure (P_{max}), then gradually decreases due to heat loss on the wall. Compared to the baseline case (with no electric field), the timing of maximum pressure is advanced by ~1 ms.

The remarkable feature in the results is the peak points in the current graph. A few mA of positive current peak is observed on the rising edge of high voltage excitation and a negative peak on the falling edge. The electrical power input on this edge point is in the order of 0.5 mJ—considering that the equivalent capacitance of high voltage electrode in constant volume chamber is approximately 10 pF, it is possible to explain that the energy is consumed to excite the electrical potential of the electrode. This energy consumption is relatively smaller than that of the spark ignition (in the order of 10 mJ) or the chemical reaction (roughly 300 J), but it drives the applicable improvement of combustion behavior.

To analyse the combustion characteristics based on obtained pressure data, the quasi-dimensional two-zone combustion model [30], [31] is adopted based on following several assumptions. First, the volume of reaction zone (i.e., thickness of flame sheath) is negligible; the model is divided into two zones—burned gas zone and unburned gas zone. Second, the pressure throughout the cylinder is uniform at any time or position. There is no difference between burned gas and unburned gas. Third, the combustion process is very rapid. The unburned mix will be fully burned immediately after the flame front passes. Fourth, properties of mixture gases are determined by the mass fraction of the composition. Fifth, each zones are treated as ideal gases with a constant specific heat.

The equation for mass and energy conservation can be written as

$$\frac{V}{m} = \int_0^{x_b} v_b \, dx + \int_{x_b}^1 v_u \, dx \tag{2.1}$$

$$\frac{U_0 - Q}{m} = \int_0^{x_b} u_b \, dx + \int_{x_b}^1 u_u \, dx \tag{2.2}$$

The equation of state can be written from the ideal gas assumption

$$Pv_u = R_u T_u \quad u_u = c_{v,u} T_u + h_{f,u} \tag{2.3}$$

$$Pv_b = R_b T_b \quad u_b = c_{v,b} T_b + h_{f,b} \tag{2.4}$$

From equations (2.1) to (2.4), the following equation is obtained

$$\frac{PV}{m} = x_b R_b \bar{T}_b + (1 - x_b) R_u \bar{T}_u \quad (2.5)$$

$$\frac{U_0 - Q}{m} = x_b (c_{v,b} \bar{T}_b + h_{f,b}) + (1 - x_b)(c_{v,u} \bar{T}_u + h_{f,u}) \quad (2.6)$$

where $\bar{T}_b$ and $\bar{T}_u$ are mean temperature of the burned and unburned gases, respectively.

$$\bar{T}_b = \frac{1}{x_b} \int_0^{x_b} T_b \, dx \qquad \bar{T}_u = \frac{1}{1 - x_b} \int_{x_b}^{1} T_u \, dx \quad (2.7)$$

Assume the unburned gas compressed isentropic process, then (2.5) and (2.6) can be derived as follows [32]

$$\frac{\bar{T}_u}{T_0} = \left(\frac{P}{P_0}\right)^{\frac{\gamma_u - 1}{\gamma_u}} \quad (2.8)$$

$$x_b = \frac{(P - P_0)V + (\gamma_b - 1)Q + (\gamma_b - \gamma_u) m c_{v,u} (\bar{T}_u - T_0)}{m[(\gamma_b - 1)(h_{f,u} - h_{f,b}) + (\gamma_b - \gamma_u) c_{p,u} \bar{T}_u} \quad (2.9)$$

$$\bar{T}_b = \left(\frac{R_u}{R_b}\right) \bar{T}_u + \frac{PV - m R_u \bar{T}_u}{m R_b x_b} \quad (2.10)$$

With equation (2.8) to (2.10), burned mass fraction can be obtained by pressure data. From the calculated burned mass fraction, 10% burn time (t_{10}) and pressure gradient near the t_{10} are defined to represent the characteristics of combustion. As presented in Figure 2.10, the best fit of pressure gradient near the 10% burn time (in the range of $5 < x_b < 15\%$) indicates excellent linearity, where the coefficient of determination R^2 is 0.998.

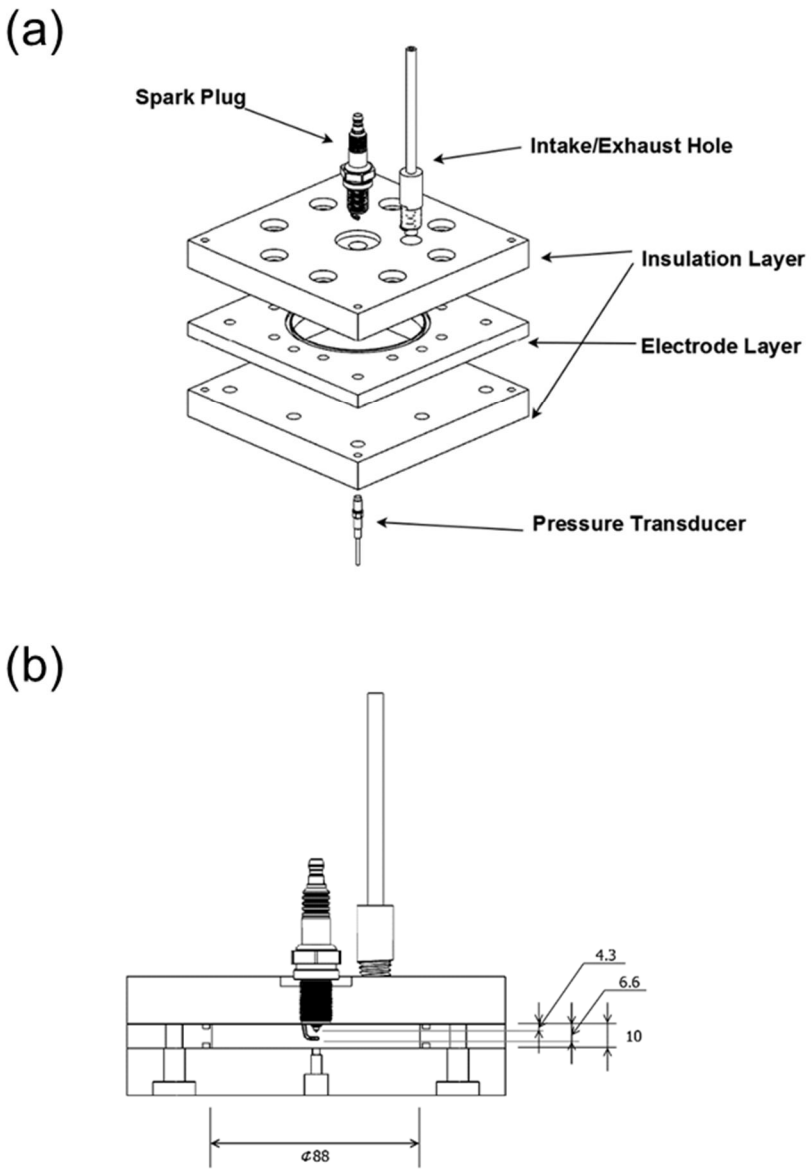

Figure 2.1 Structure of the constant volume chamber (a) exploded view; (b) cutaway view.

Figure 2.2 Picture of the constant volume chamber.

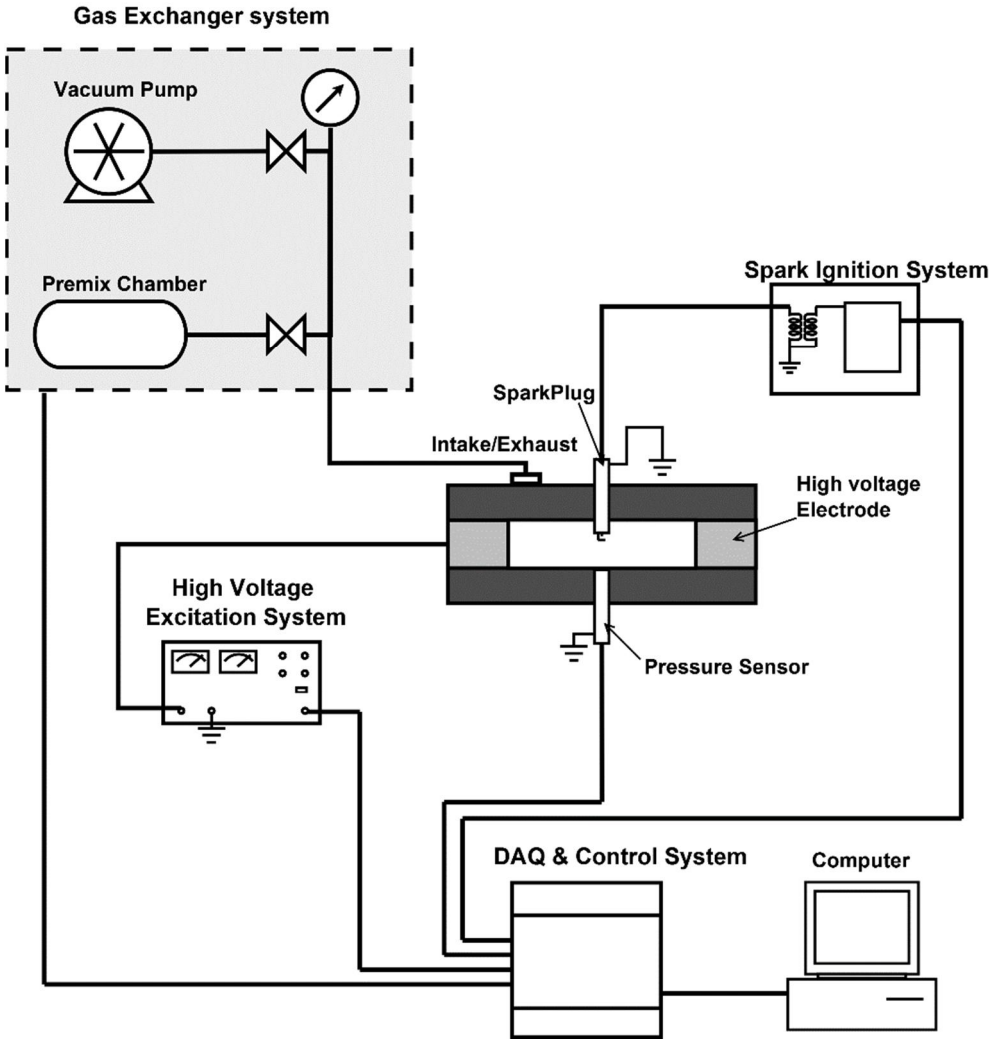

Figure 2.3 Schematics of experimental setup.

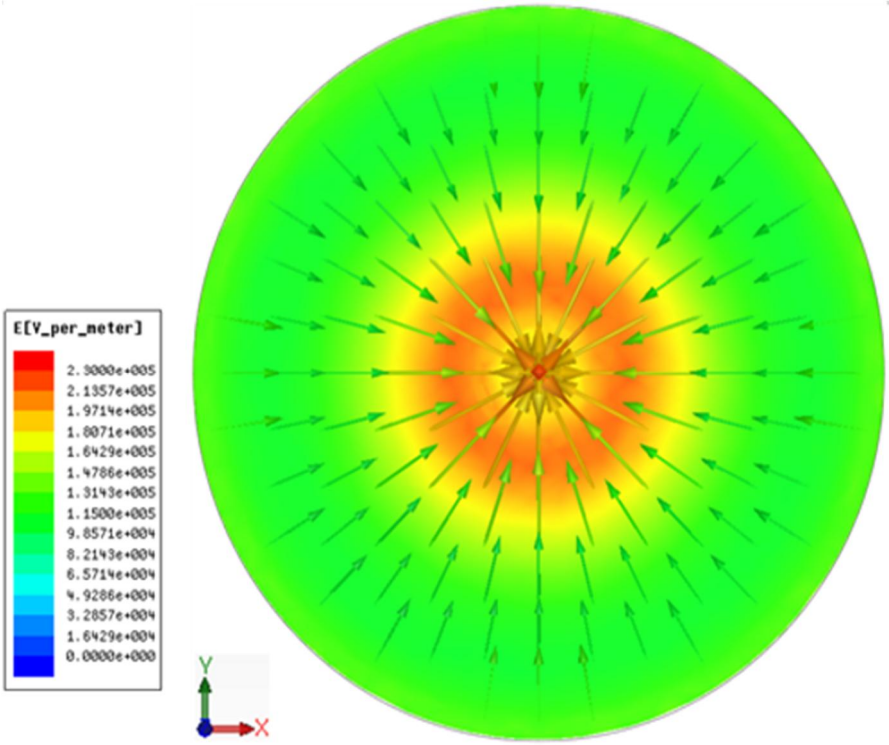

Figure 2.4 Simulation result of electric field inside the chamber. (V_e = -7kV, Top view)

Table 2.1 Specifications of the developed DAQ/control system.

Parameter	Value
Data acquisition	
Sampling rate [kS/s]	100
ADC resolution [bits]	16
Control	
Output current range [mA]	±10
Output voltage range [kV]	±10
Output voltage error [kV]	< 0.05
Settling time [ms] (to 99%)	< 0.2
Timing resolution [ms]	0.1
Experimental condition	
Dimension of chamber [mm]	Ø88×h10
Initial temperature [°C]	85±2
Initial pressure [bar]	2±0.01
No. of repetitions per conditions	> 8

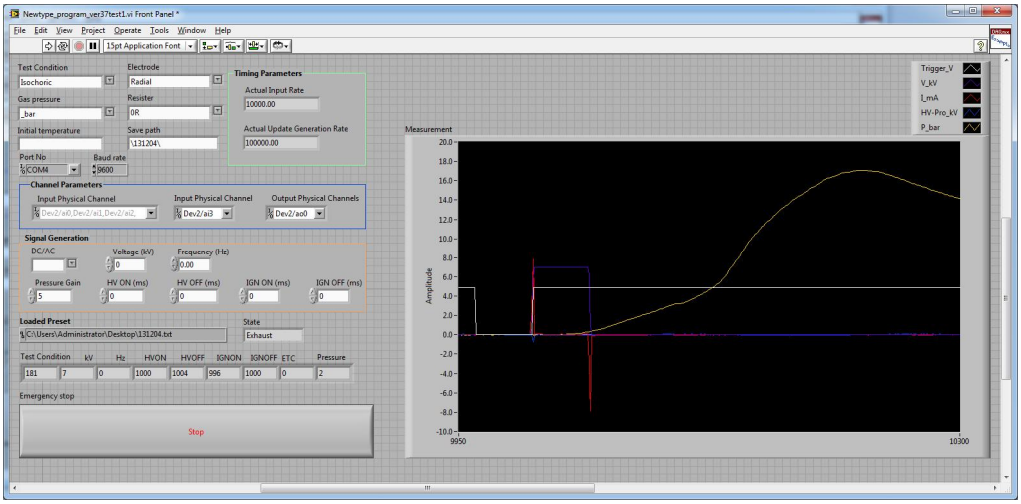

Figure 2.5 Screenshot of developed monitoring software.

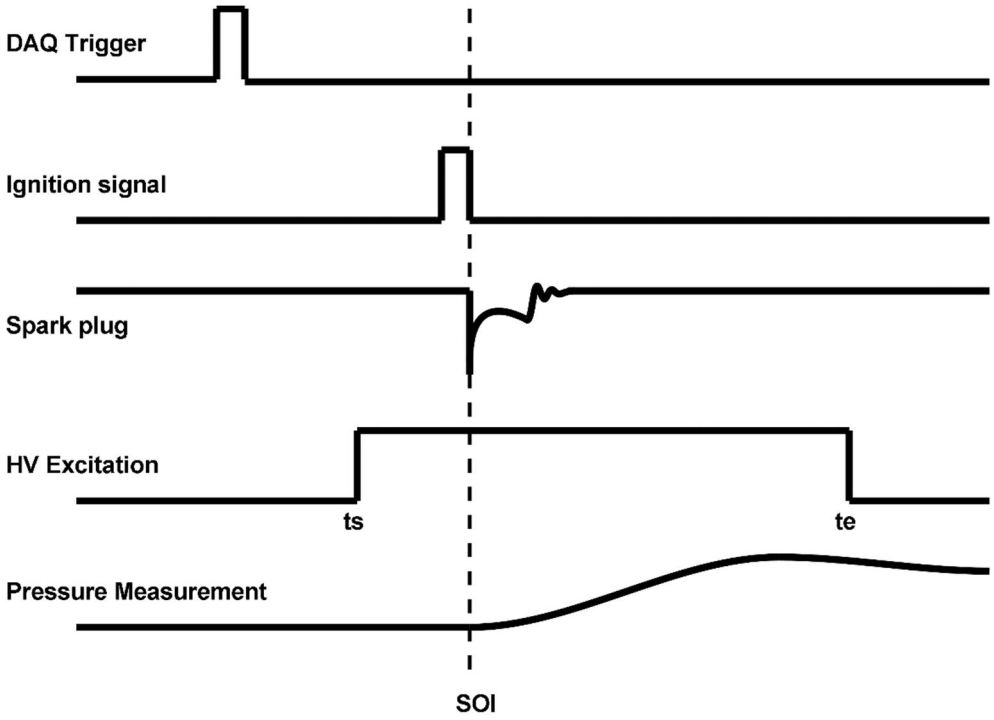

Figure 2.6 Timing chart of experiment. SOI is set as the origin and the timings including high voltage excitation, measurements are synchronized to the SOI.

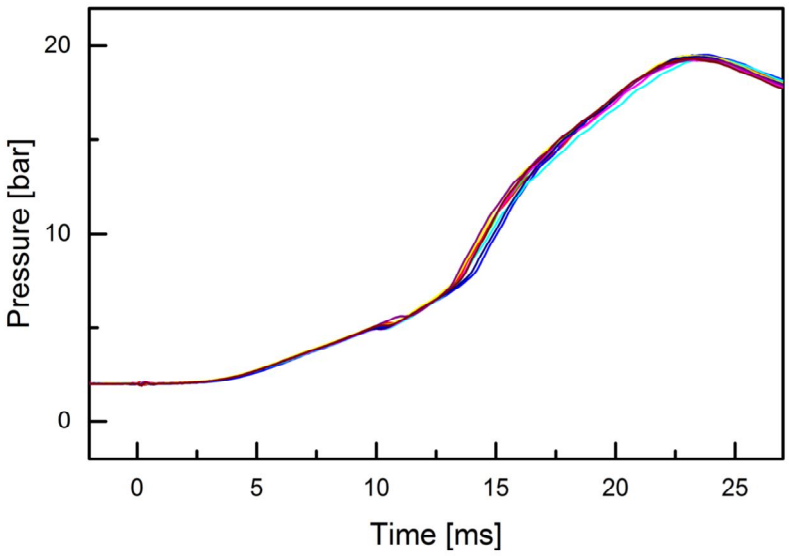

Figure 2.7 Shot-by-shot variation of experiments without electric field.

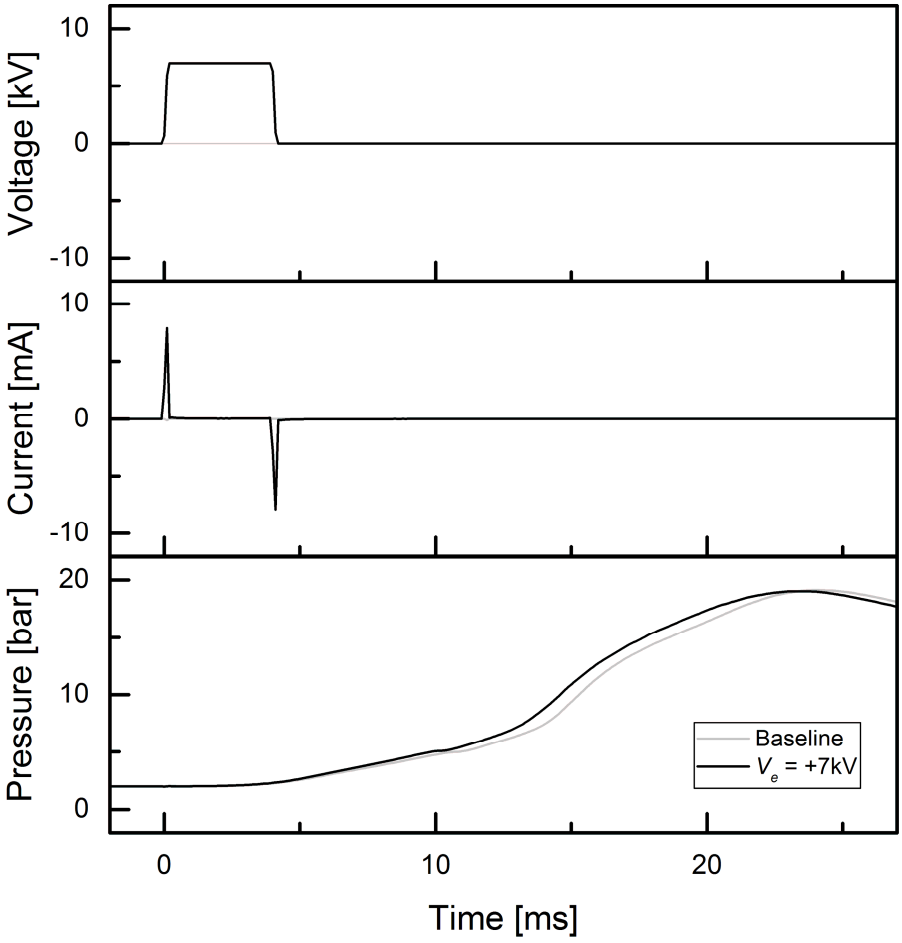

Figure 2.8 Voltage, current, and pressure versus time at the voltage profile of t_s = 0 ms, t_e = 4 ms, and V_e = +7 kV.

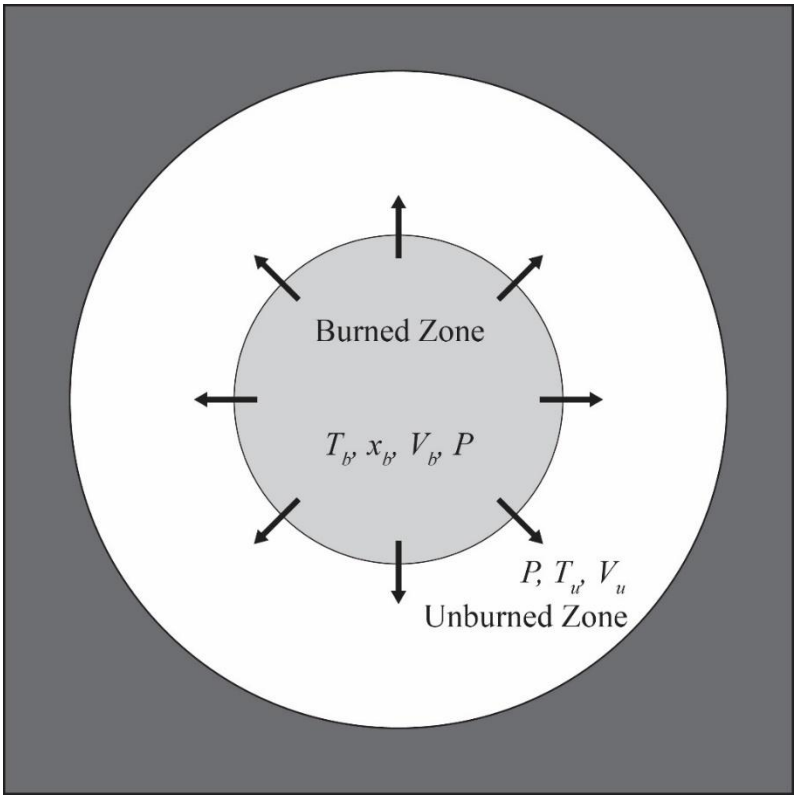

Figure 2.9 Schematic diagram of the two-zone model.

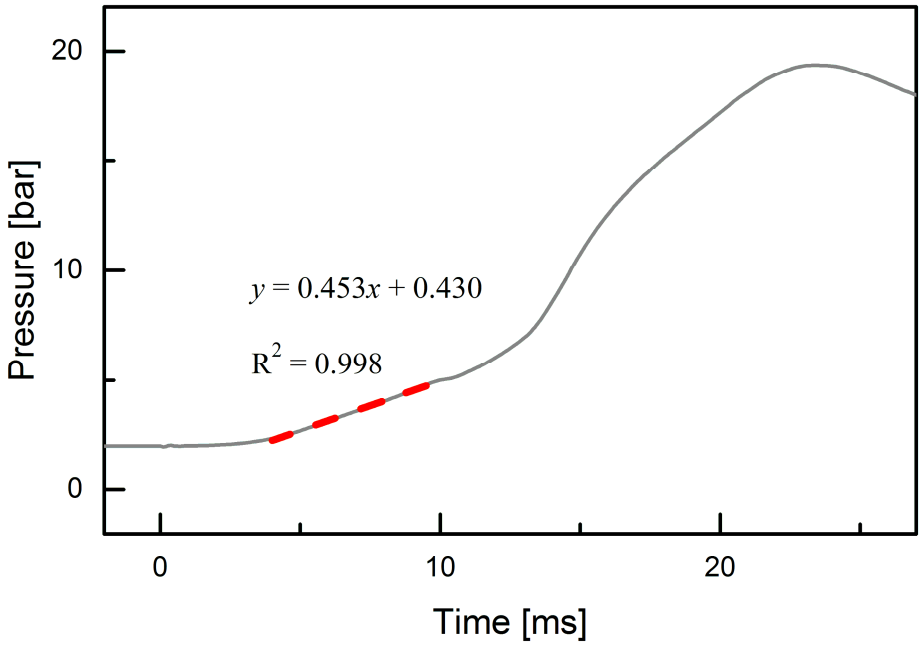

Figure 2.10 Definition of pressure gradient near t_{10}.

Chapter 3. Effects of Positive DC Electric Field Excitation

According to the previous studies, the affection of the ionic wind effect is maximized in negative DC electric field (i.e., the electric field and the flame propagation are aligned in the same direction) [4], [9]. However, the effects of a positive DC (i.e., the directions are opposite) electric field, as shown in Figure 3.1, have received little attention. Furthermore, it is obvious that the timing and duration of the excited electric field are critical factors in establishing characteristics of the transient flame. Nonetheless, few researches have paid attention to the factors involved. Most of the previous studies having focused on a continuous electric field [12], [14]. This chapter, therefore, aims at observing the effect of duration of positive electric field by varying the start time and the end time of excitation.

3.1 Effects of Timing Sweep

3.1.1 Effect of end time

Figure 3.2 shows the timing diagram of the full range sweep experiments for investigating the effect of the end time. The experiments are repeated 12 times for each condition. The start time of electric field excitation, t_s, was fixed at 800 ms before SOI, and the end time, t_e, was varied between 0 ms (SOI) and 30 ms with steps

of 2 ms. That is to say, the electric field was applied sufficiently before SOI, and the duration varies. The excitation voltage, V_e, was set to +7 kV to maintain consistent combustion condition. If the excitation voltage is greater than 7 kV, the electric field intensity at the end of combustion period becomes large enough to cause the arc discharge. Initial condition of the combustion is set as 2bar, 85°C, and stoichiometric air fuel mixture.

The change of the flame propagation characteristics with respect to the end time of electric field excitation were investigated. The flame propagation characteristics including maximum pressure, 10% burn time, and pressure gradient near the 10% burn time are plotted in Figure 3.3.

For t_e = 0 ms, flame propagation characteristics show no difference from the baseline. This result confirms that the electric field does not have an affection before SOI. In previous researches, it was established that non-equilibrium plasma discharge, such as gliding arc discharge [33] and dielectric barrier discharge [15], [34], in the unburned zone can produce fuel fragments and improve the combustion characteristics and delay of ignition. However, in the present study, the effect of positive DC electric field is not observed in this region.

Along with the t_e increases, improvements of these flame propagation characteristics are observed. The enhancement of combustion characteristics is defined as follows [13]:

$$\Delta C = \frac{C - C_0}{C_0} \times 100\ [\%] \quad (3.1)$$

where C is the values of combustion characteristic in case of the electric field excitation, and C_0 is that of baseline condition. When t_e = 6 ms, then t_{pmax}, t_{10}, and dP/dt are enhanced up to -2.45%, -4.80%, and 7.67%, respectively. As t_e is later than 6 ms, the saturation point, at which additional enhancement on flame propagation is negligible, is observed. This result implies that the effect of positive DC electric field on flame enhancement occurs within the first few milliseconds after SOI. On the other hand, the excitation on other periods (i.e., before SOI or after initial period) is less effective.

3.1.2 Effect of start time

The effect of start time was inspected, as outlined in Figure 3.4. The end time of excitation, t_e, was set to 1000 ms after SOI, and the start time, t_s, was varied between 0 ms (SOI) and 30 ms with steps of 2 ms; the electric field excitation was retained until the combustion ends, and duration was shortened. The excitation voltage V_e was set to +7 kV in the same manner as in Chapter 3.1.1. Initial condition of the combustion is set as 2bar, 85°C, and stoichiometric air fuel mixture.

The relationship between the flame propagation characteristics and the start time is depicted in Figure 3.5. When t_s = 0, dP/dt near the t_{10}—related to the burning rate—is increased by 9.65%. As the burning rate rises, t_{pmax} and t_{10} are increased by -2.57% and -4.70%, respectively. These improvements gradually begin to decrease as t_s is delayed and the duration of electric field excitation is shortened. Finally, when ts is later then 4ms, the results became indistinguishable from baseline. This result further

supports that the effect of electric field on flame enhancement is limited the initial period of combustion.

3.2 Boundary of Effective Regime

The result of the full-time sweep experiments (described in previous chapter) confirms that the electric field exerts an effect only in the very short period of flame propagation. To determine the more precise boundary of the effective regime, additional experiments limited to the range of early stage were performed. The experiments are repeated at least eight times for each condition.

3.2.1 Boundary of end time

The timing diagram to determine the end time of the effective regime is shown in Figure 3.6. Since the former experiments affirm the insignificant effect of electric field excitation on combustion before SOI, its start time (t_s) was fixed at SOI. The end time (t_e) was adjusted up to 4ms at 0.5-ms intervals; in other words, the duration of excitation was varied between 0.5 ms (t_s = 3.5ms) and 4 ms (t_s = 0ms).

As the duration of high voltage excitation increases, the timings—including t_{pmax}, t_{10}—are advanced and pressure gradient dP/dt increases. However, when t_e is later than 2.5ms, the saturation point, at which increased duration has negligible additional enhancement, is shown in Figure 3.8.

3.2.2 Boundary of start time

Figure 3.9 shows the timing diagram of experiments varying the start time of electric field excitation in order to identify the boundary of effective regime. As mentioned in Chapter 3.1.2, the influence of the electric field is negligible when excitation is later than 4ms. Thus, t_e was fixed at 4 ms, and the duration was varied between 4 ms (t_s = 0 ms) and 0.5 ms (t_s = 3.5ms).

As shown in Figure 3.11, enhancement of combustion characteristics including t_{pmax}, t_{10}, and dP/dt are maximized to -3.05%, -5.76%, 12.25% respectively. However, these enhancements decrease as t_s is delayed, and approach baseline when t_s is later than 2.5 ms. These results consistently show that the effect of positive DC electric field on flame enhancement occurs within only ~2.5 ms.

3.3 Observation of Current Flow

The measured history of current flow through the high voltage is plotted in Figure 3.12. The experimental condition was fixed at V_e = +7 kV, t_s = -800 ms, and t_e = 30 ms; briefly, positive DC potential of 7 kV was continuously applied through the whole combustion process. The three distinct regimes in the result will be analyzed in consecutive order.

The first regime, before SOI, shows negligible improvement of combustion.

Nonetheless, in this regime, a stable current flow of approximately 10 μA was measured. Regardless of flame propagation, this weak current is explained as follows: (1) dark discharge due to the ionization of gas molecules (2) leakage current caused by imperfect insulation and a shunt resistor used monitor the system.

The second is the effective regime of the positive DC electric field. In this regime, the current gradually increases up to 30 μA as the combustion progresses. Considering that ~10 μA of current is consumed to maintain the electric field even before combustion, an additional 20 μA of ionic current flows due to the flame propagation. The power drawn from the electric field is ~200 mW; ~0.5 mJ was consumed during this regime. Compared with the chemical energy (~300 J) of flame, relatively small electrical energy dramatically affects the combustion process.

The third regime comes after the effective regime. In this regime, a continuous trend of gradual increasing, as shown in the past period (i.e., effective regime), is maintained. This phenomenon is interpreted as an ionic current because the flame front approaches the electrode with respect to the progress of combustion. As a consequence, it features the peak value (~200 μA). Nonetheless, no noticeable change of combustion is observed.

3.4 Concluding Remarks

The effects of the positive DC electric field timing on the flame propagation were studied experimentally. To assess the effect of the electric field, combustion

characteristics calculated from the measured pressure history were evaluated by varying the timing of electric field excitation, including the start and the end time. The effective regime for the positive DC electric field is identified in the initial period, whereas it appears less effective in other periods of combustion. The positive DC electric field affects only within 2% from SOI (based on mass fraction rate). Despite this fact, these improvements are observed near the 10% burn time. Once the enhancement of combustion speed arises in the effective regime, it is maintained even after disconnecting the high voltage. In this effective regime, the additional current of approximately 10 μA is measured. After this regime, there is progressive increase of the current flows due to the ionic current, whereas the additional enhancements are negligible. Consequently, the relatively low (lower than 1% of chemical energy) electrical energy drastically affects the combustion characteristics. The experiment results reveal that the electric field accelerates the growth of flame kernel, and it raises the combustion speed.

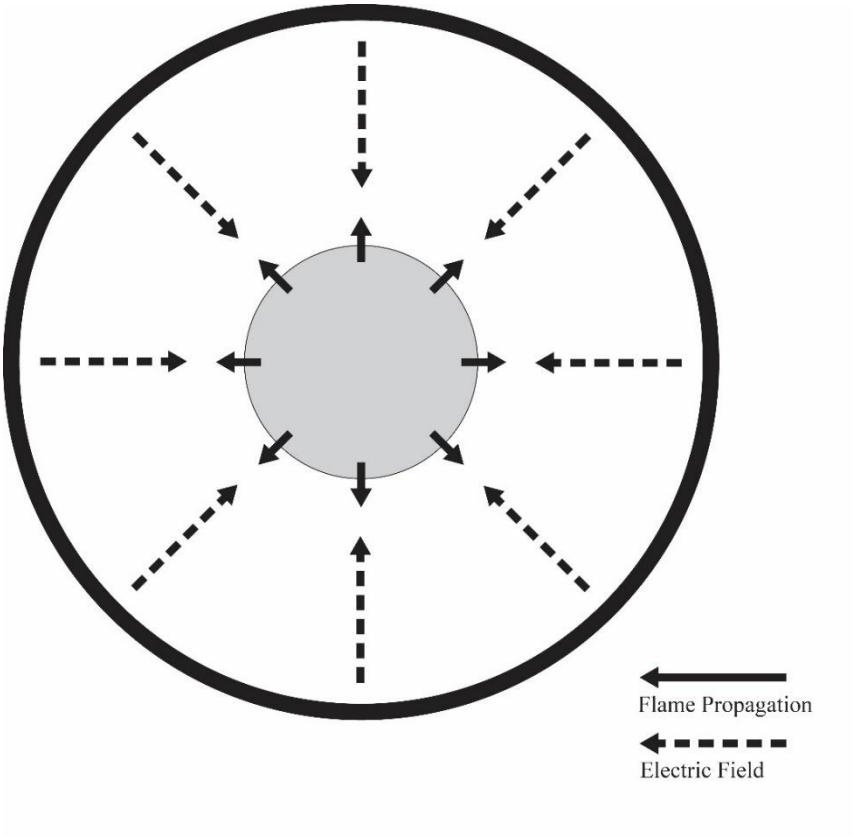

Figure 3.1 Directions of electric field and flame propagation when positive potential is applied.

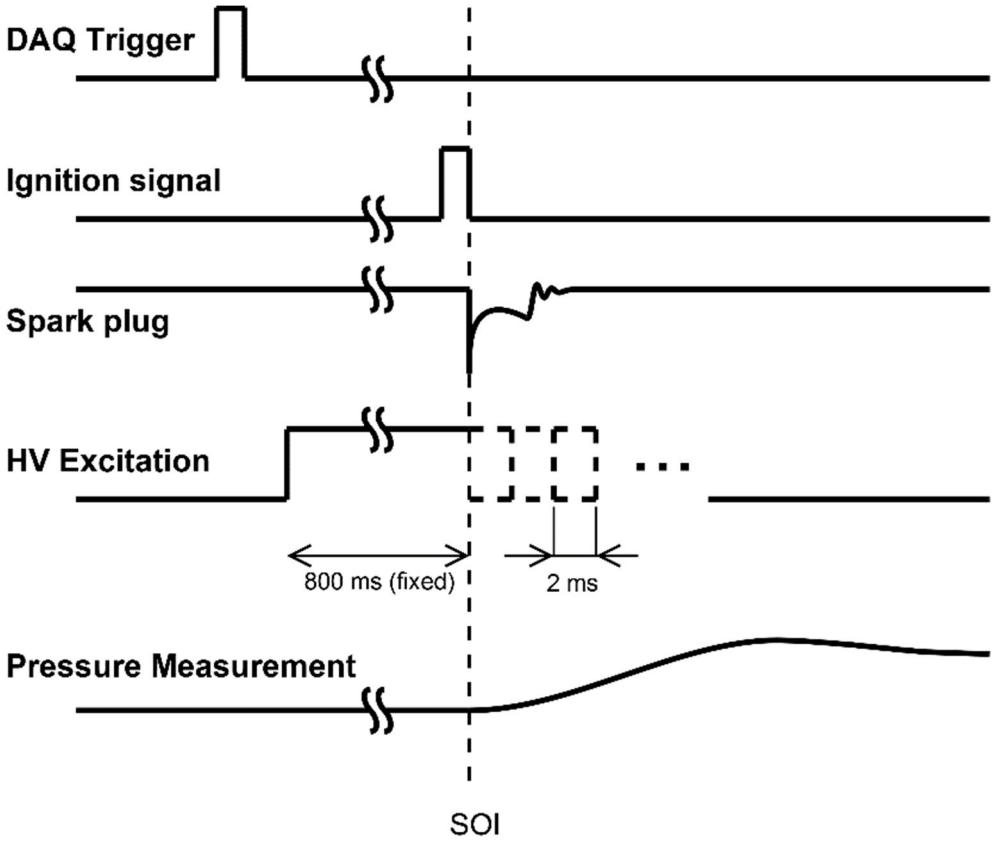

Figure 3.2 Timing chart of the timing sweep experiments by varying t_e at V_e = +7 kV and t_s = -800 ms.

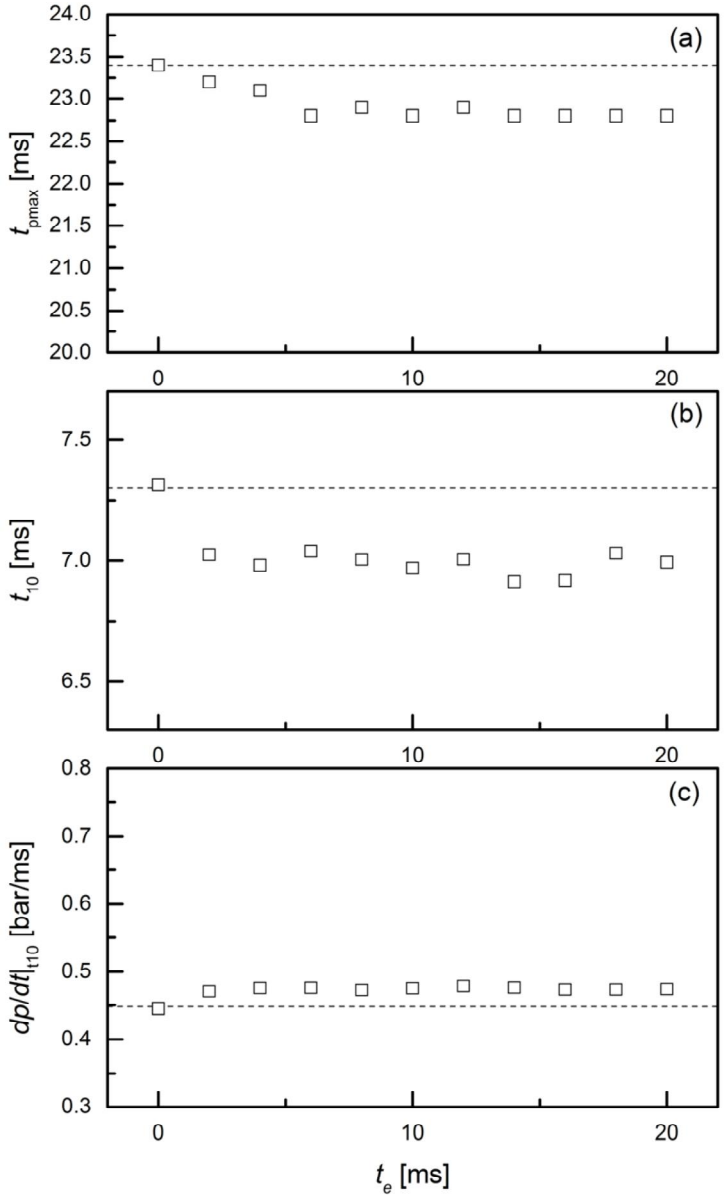

Figure 3.3 Flame propagation characteristics as a function of t_e (t_s is fixed at 800 ms before SOI). (a) t_{Pmax}; (b) t_{10}; (c) dP/dt.

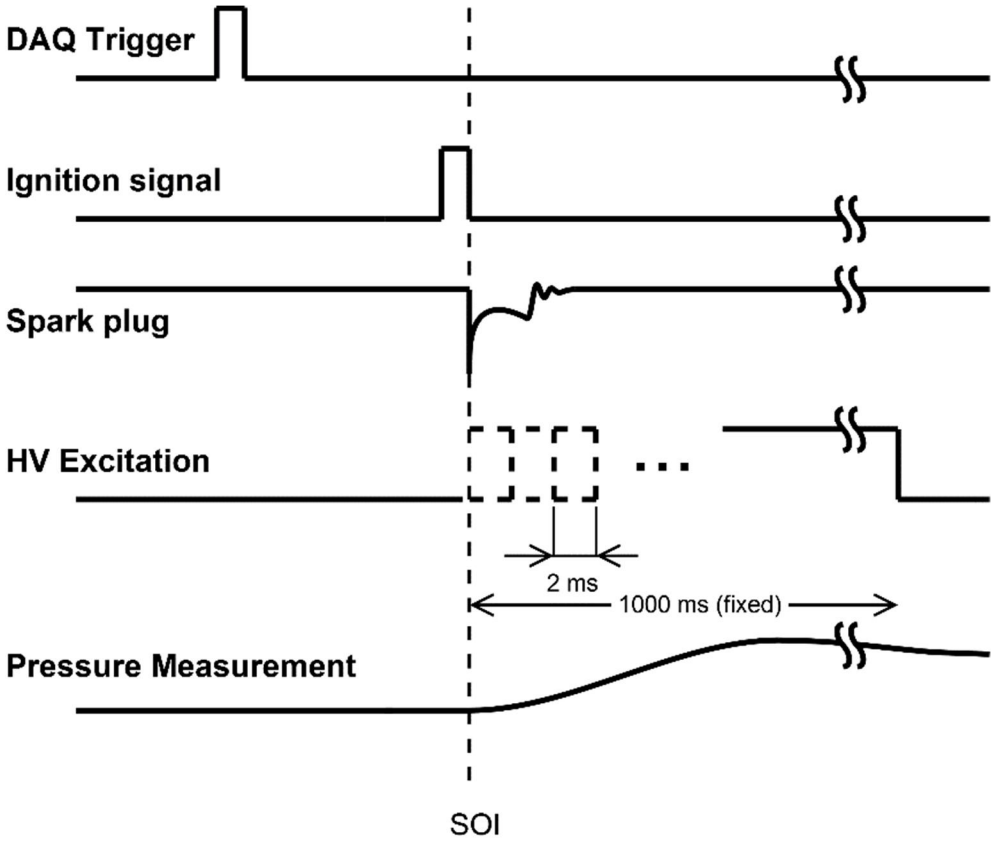

Figure 3.4 Timing chart of the timing sweep experiments by varying t_s at V_e = +7 kV and t_e = 1000 ms.

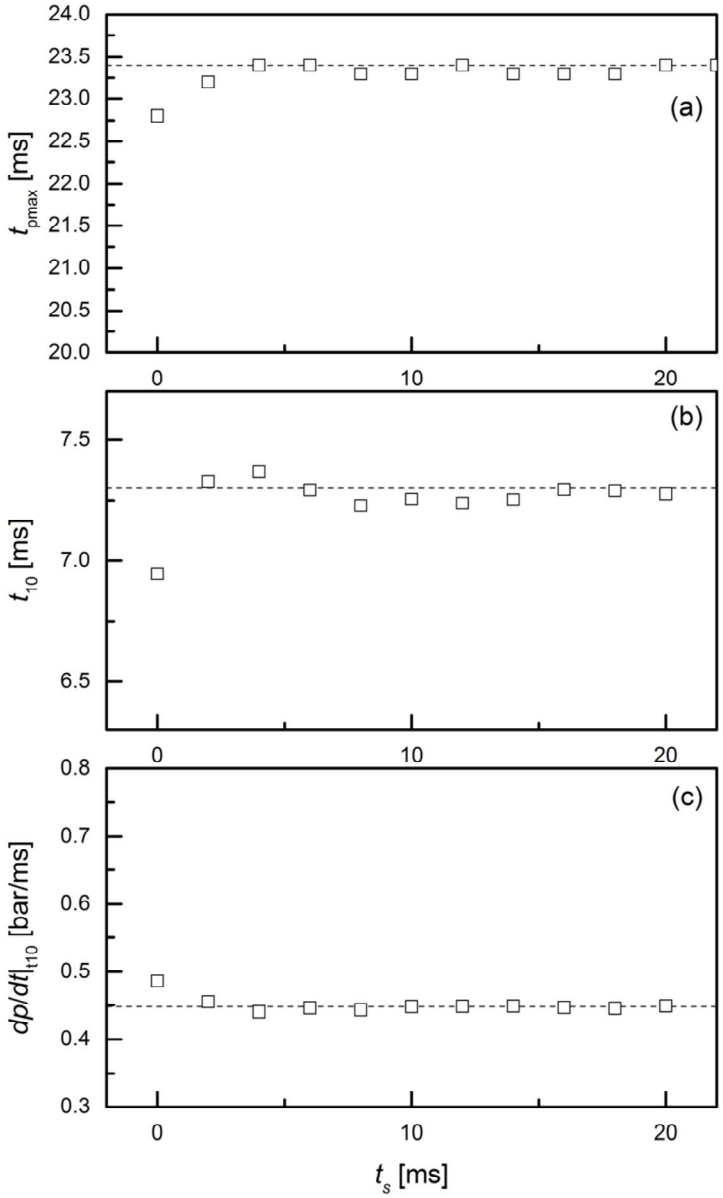

Figure 3.5 Flame propagation characteristics as a function of t_s (t_e is fixed at 1000 ms after SOI). (a) t_{Pmax}; (b) t_{10}; (c) dP/dt.

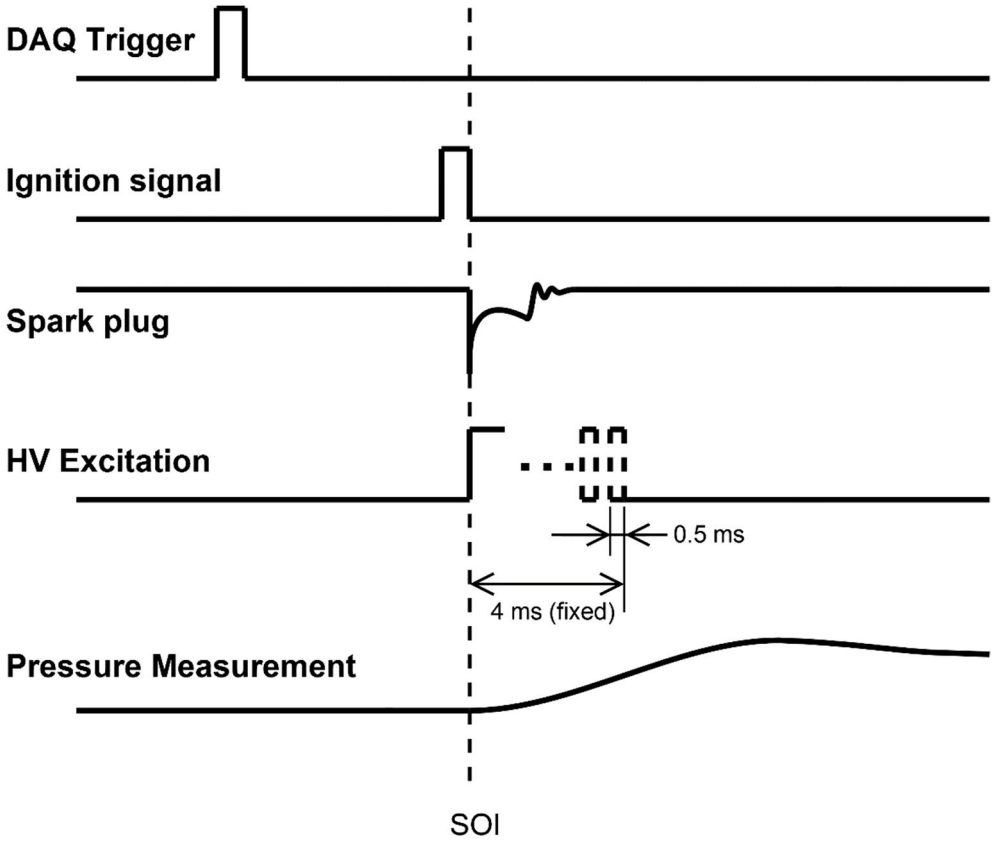

Figure 3.6 Timing chart for identification of effective regime by varying t_e within the flame initiation period. V_e and t_s are fixed at = +7 kV and SOI respectively.

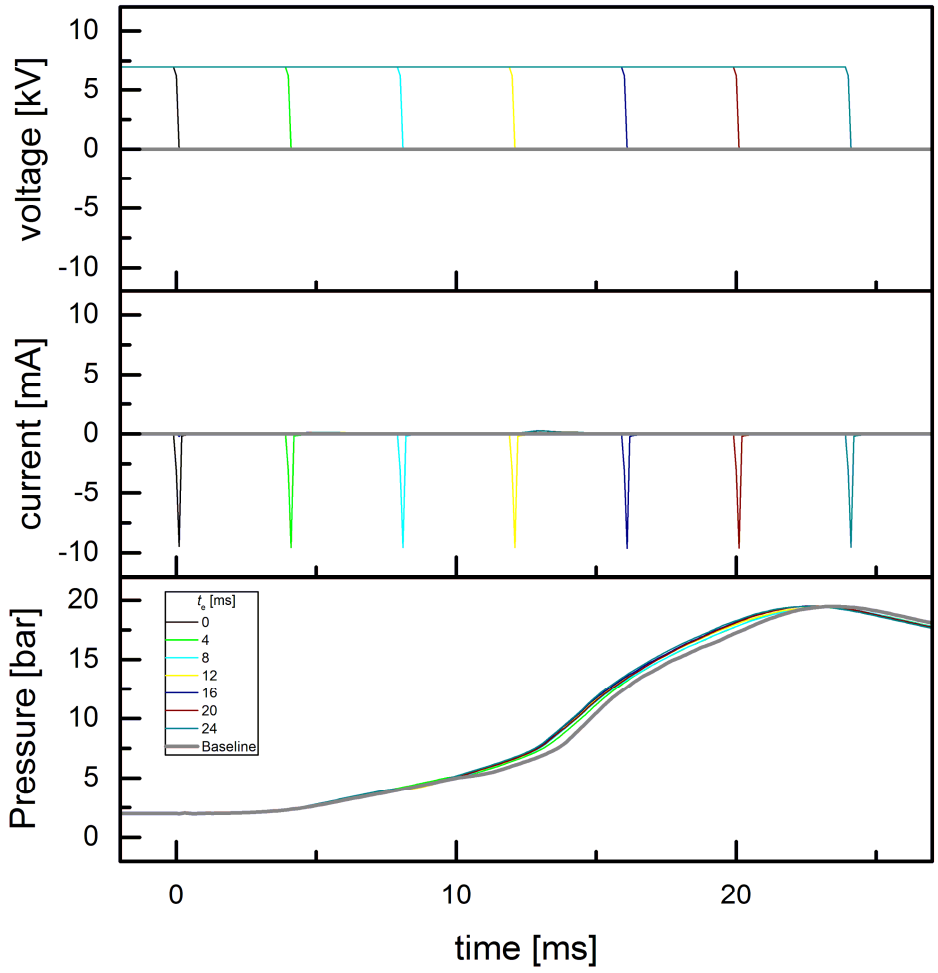

Figure 3.7 Voltage, current, and pressure versus time by varying end time. (V_e = -7 kV and t_s = -800 ms).

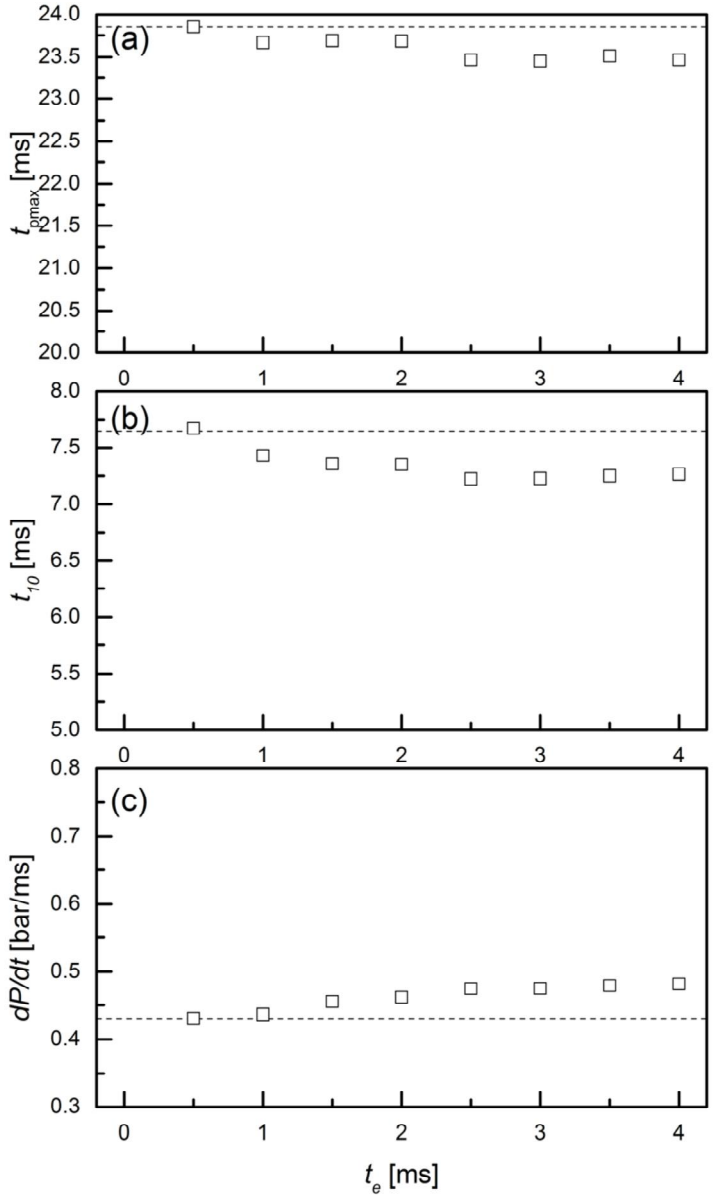

Figure 3.8 Flame propagation characteristics as a function of t_e (t_s = 0 ms and V_e = +7 kV). (a) t_{Pmax}; (b) t_{10}; (c) dP/dt.

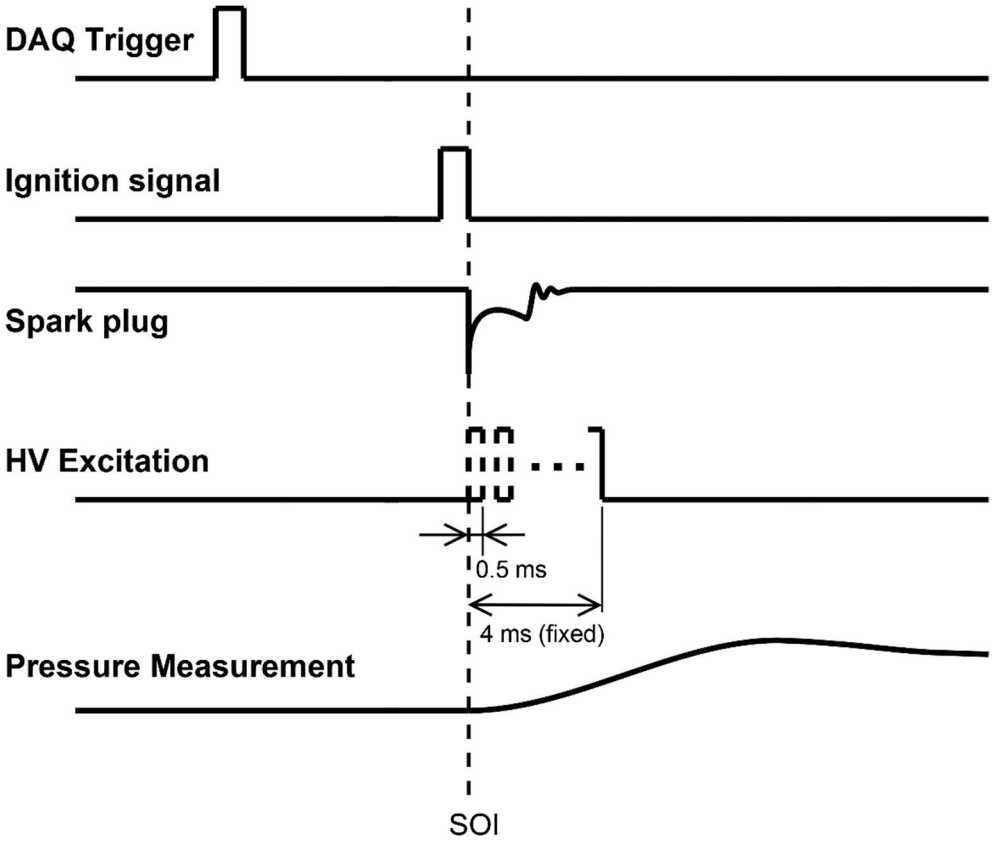

Figure 3.9 Timing chart for identification of effective regime by varying t_s at flame initiation duration. V_e and t_e are fixed at = +7 kV and 4 ms respectively.

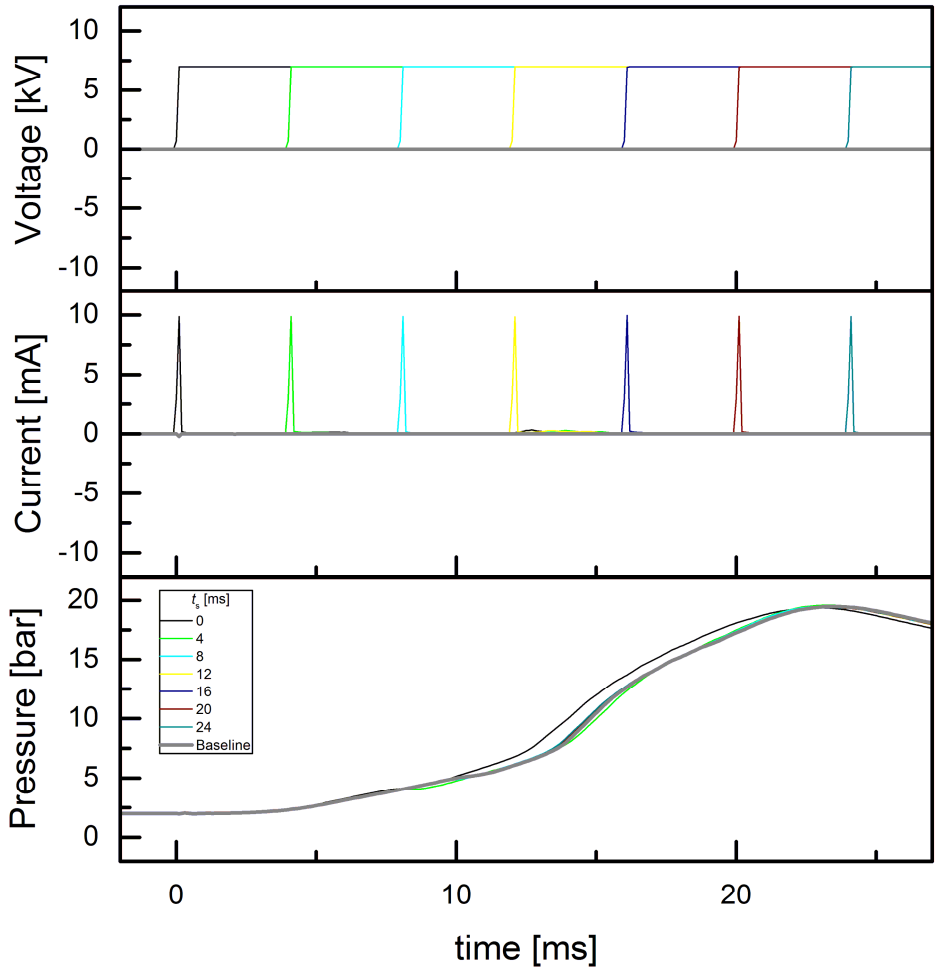

Figure 3.10 Voltage, current, and pressure versus time by varying start time. (V_e = -7 kV and t_e = 1000 ms).

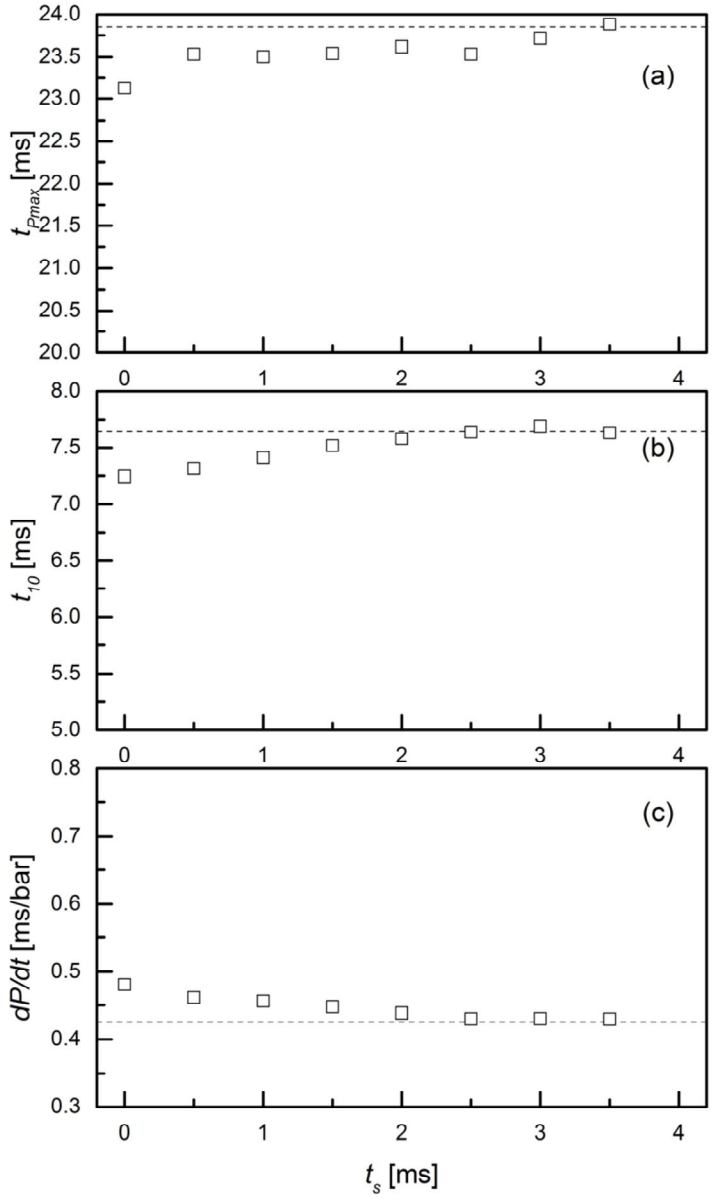

Figure 3.11 . Flame propagation characteristics as a function of t_s (t_e = 4 ms and V_e = +7 kV) (a) t_{Pmax}; (b) t_{10}; (c) dP/dt.

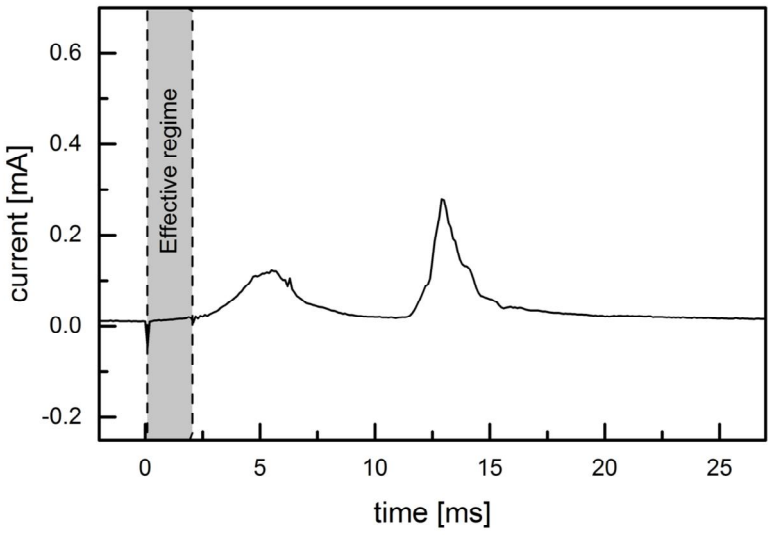

Figure 3.12 History of current flow when positive DC electric field is applied (t_s = -800 ms, t_e = 30 ms, and V_e = +7 kV).

Chapter 4. Effects of Negative DC Electric Field Excitation

The effect of positive DC electric field was observed in Chapter 3, and the result shows that the positive DC electric field influenced the growth of the flame kernel. In this chapter, the affection of negative DC electric field on flame propagation is assessed. When negative potential is applied to the high voltage electrode, the electric field and the flame propagation are aligned in the same direction, as shown in Figure 4.1

4.1 Effects of Timing Sweep

4.1.1 Effect of end time

Figure 4.2 shows the timing diagram of experiments performed to confirm the relationship between the combustion speed and the end time of negative DC electric field excitation. The experiments are repeated 13 times for each condition. The excitation voltage, V_e, was fixed at -7 kV; thus, compared to the condition of Chapter 3, the intensity of electric field is equivalent to it, whereas the polarity is opposite to it. The start time of electric field excitation, t_s, is fixed at -800 ms, and the end time, t_e, was varied in the range of SOI to 30 ms. Initial condition of the combustion is set as 2bar, 85°C, and stoichiometric air fuel mixture.

The results of experiments are plotted in Figure 4.3. The pressure history shows that the peak pressure and its timing gradually increase as the t_e is delayed (i.e., the duration of excitation is extended). The notable change of trend was observed after 12 ms (x_b > 20%); the current flow rapidly increases in O(1 mA), and the peak pressure value changes dramatically.

4.1.2 Effect of start time

The effect of start time was inspected, as shown in Figure 4.4. The end time of excitation t_e was fixed at 1000 ms after SOI, and the start time t_s was varied; in other words, the electric field excitation was retained until the completion of the combustion, and the duration of excitation was shortened. An excitation voltage of – 7 kV was applied to the high voltage electrode inside the chamber.

The measured voltage, current, and pressure history versus time are presented in Figure 4.5. Similar to the result of the previous subsection, improvements of the pressure rise gradually begin to diminish with respect to the t_e—that is, duration of high voltage excitation is shortened. The timing of notable points, mentioned above (experiments with respect to the t_s), was not clear. This is because the 20% burn times (x_b = 20%) were different for each experiment, as the electric field affects the initial process of combustion (0 < t < 12 ms).

4.1.3 Identify regimes by observing the current

To identify the regimes, the representative samples are depicted in Figure 4.6. The experimental condition of red line is t_s = 800 ms and t_e = 12 ms; that of blue line is t_s = 800 ms and t_e = 26 ms; and the magnified current graph of the blue line is plotted in Figure 4.7. Two different regimes depending on the current flow are identified.

The first is named sub-regime I. In this regime, the current flow grows slightly as the combustion progresses, and saturates (~200 μA) when mass burn fraction x_b is 20%. In sub-regime II, beyond the saturation point, current sharply increases again, and two peak values (~1 mA and ~1.5 mA, respectively) are discovered. The history of pressure shows indistinguishable curves until 16ms (i.e., burned mass fraction is 75%), and drastic increase of pressure near the last period of combustion (x_b = 85%) is observed.

4.2 Sub-regime I

As mentioned above, the measured current shows the saturated regime at 12 ms (i.e., x_b = 20%). Additional experiments were performed to determine the effects of negative DC electric field in the sub-regime I. The graphs of the voltage, the current, and the pressure by varying the end time of excitation within the sub-regime I are plotted in Figure 4.8. The start time of electric field and the excitation voltage are

fixed at -800 ms and -7 kV, respectively. The pressure history shows the slightly increased maximum pressure (p_{max}) and the advanced maximum pressure time (t_{pmax}) when the negative potential is applied. The electrical power consumption calculated by the measured voltage and current in this regime is approximately 1 W.

The change of flame propagation characteristics in terms of the end time is plotted in Figure 4.9. For t_e = 0 ms, flame propagation characteristics are showing no difference from the baseline. That is to say, the negative DC electric field before SOI is ineffective. Considering the result of positive DC electric field mentioned in Chapter 3, it is concluded that there is no effect of DC electric field, irrespective of the polarity of excitation voltage. According to the delay of the t_e (i.e., extension of the duration of applied electric field), linear increase of flame propagation characteristics is observed.

4.3 Sub-regime II

Sub-regime II is beyond the saturation point of current, from 12 ms to the end of combustion (i.e., x_b > 20%). In this regime, the current shows sharp increase up to 1 mA, as mentioned above. The electrical power consumption in sub-regime II is up to 10 W, tens of times higher than that of sub-regime I.

Figure 4.10 illustrates the history of the measured voltage, current, and pressure. The experiment conditions were set as V_e = -7 kV and t_e = 1000 ms (i.e., the excitation was retained until the end of combustion). The pressure history shows a drastic increment of peak pressure and the advance of its timing near the last period of

combustion. For example, when t_s = 18 ms, the timing at which the pressure history begins to separate from the baseline is 20ms; when t_s =12 ms, the timing of separation occurs at 18 ms. In other words, despite the t_s being advanced by 6 ms, the timing of separation is advanced by only 2 ms. However, this enhancement diminishes when ts > 20 ms. Although the measured data shows the current flow after 20 ms from SOI, no noticeable changes are observed.

Figure 4.11 shows the change in the flame propagation characteristics by varying start time of excitation, t_s. For t_s = 12 (i.e., excited in full-duration of regime III), The maximum pressure, the timing of maximum pressure, and the pressure gradient near the end of combustion are improved by up to 7.9%, -6.1%, and 59.7%, respectively. These improvements decrease linearly along with the retardation of t_s (i.e., duration of excitation is shortened.). Finally, when t_s > 20 ms, the enhancements are diminished, and the pressure history shows no difference from baseline, as mentioned in Figure 4.10. These results confirm that the electric field is effective in regime III within 12 < t < 20 ms.

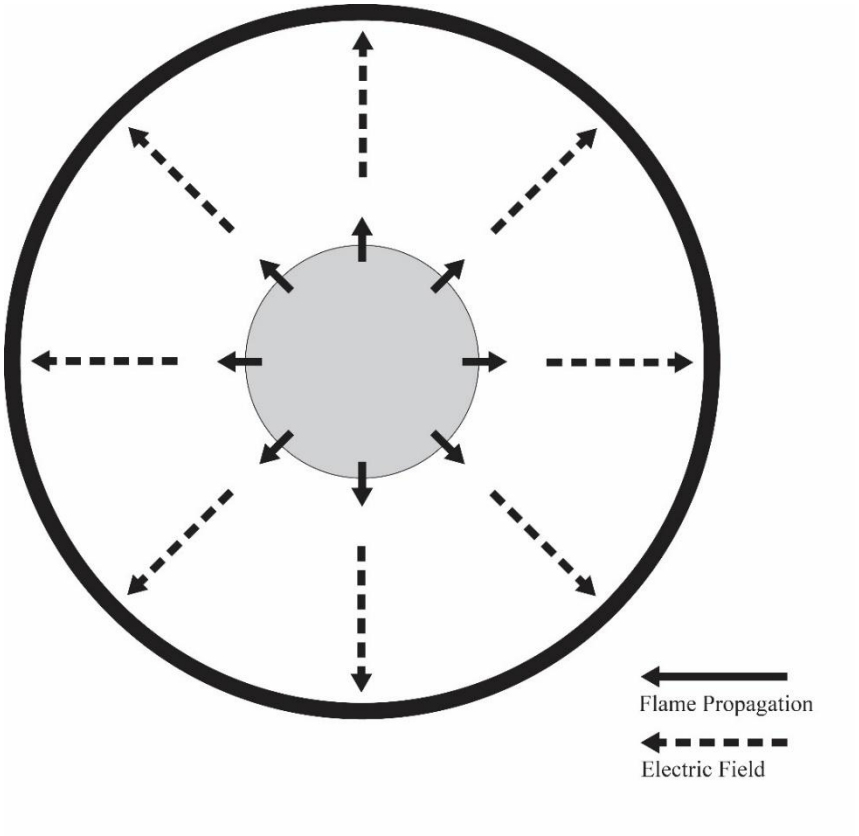

Figure 4.1 Directions of electric field and flame propagation when negative potential is applied.

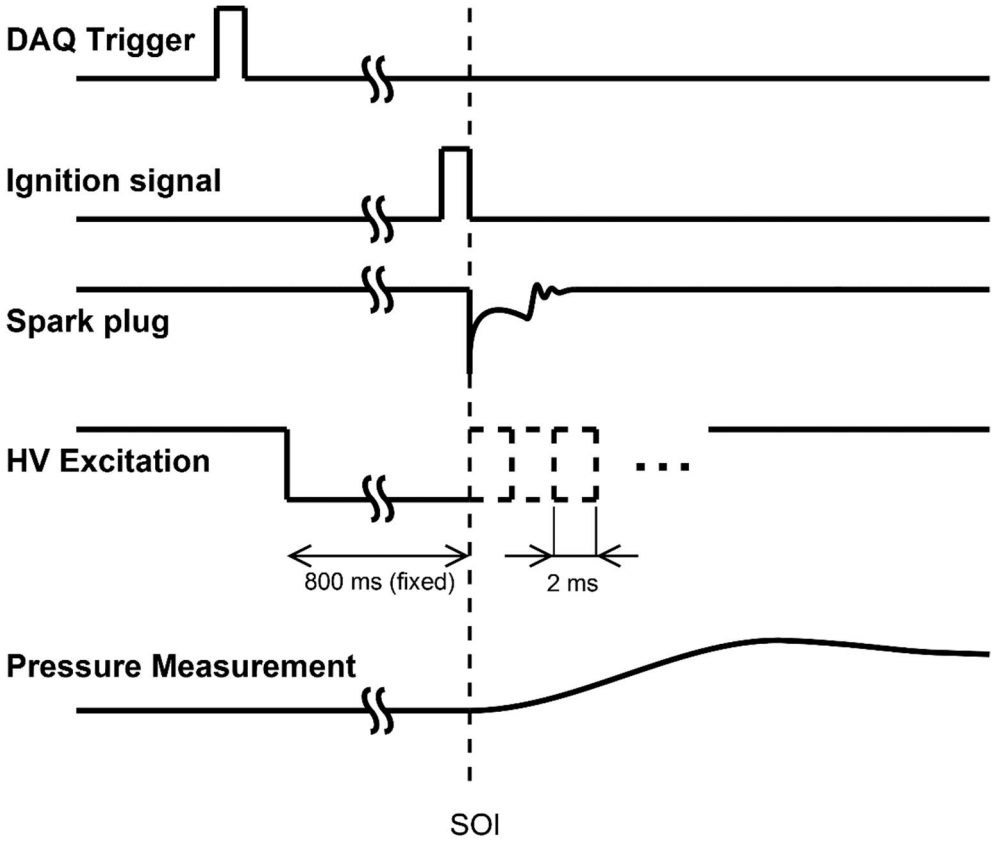

Figure 4.2 Timing chart of timing sweep experiment by varying t_e at V_e = -7 kV and t_s = -800 ms.

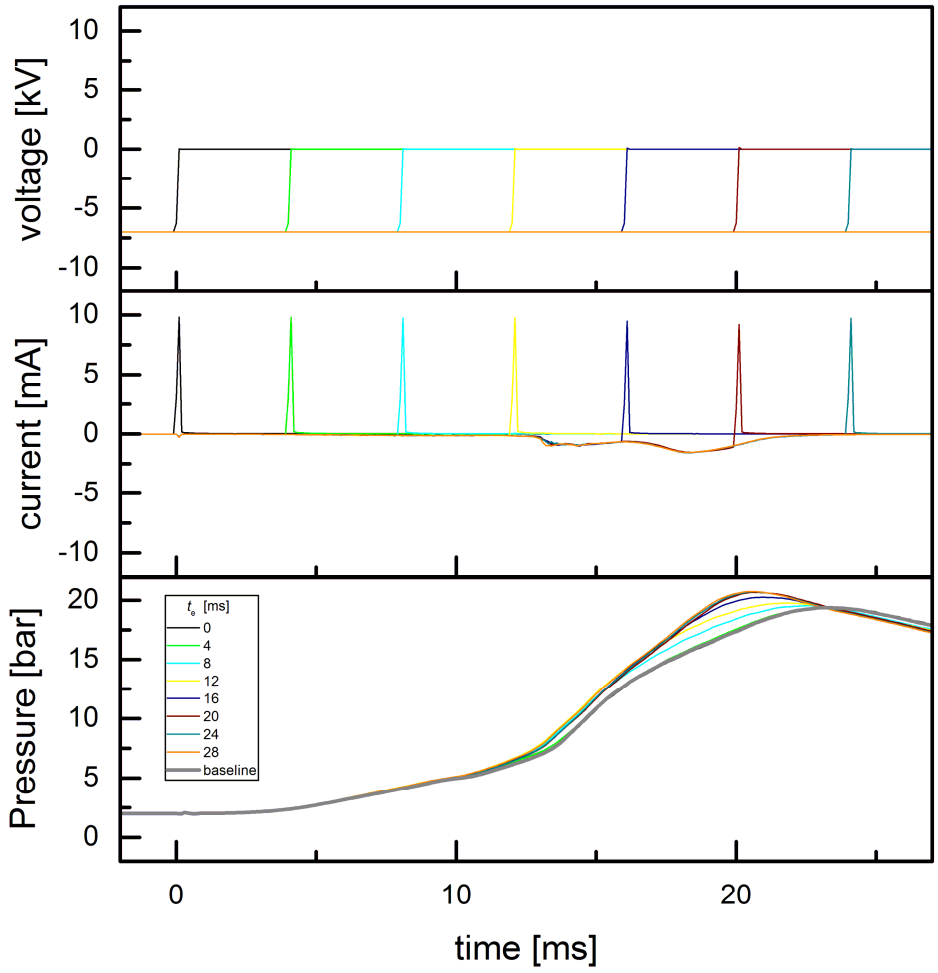

Figure 4.3 Voltage, current, and pressure versus time by varying t_e. V_e and t_s are set to -7 kV and -800 ms, respectively.

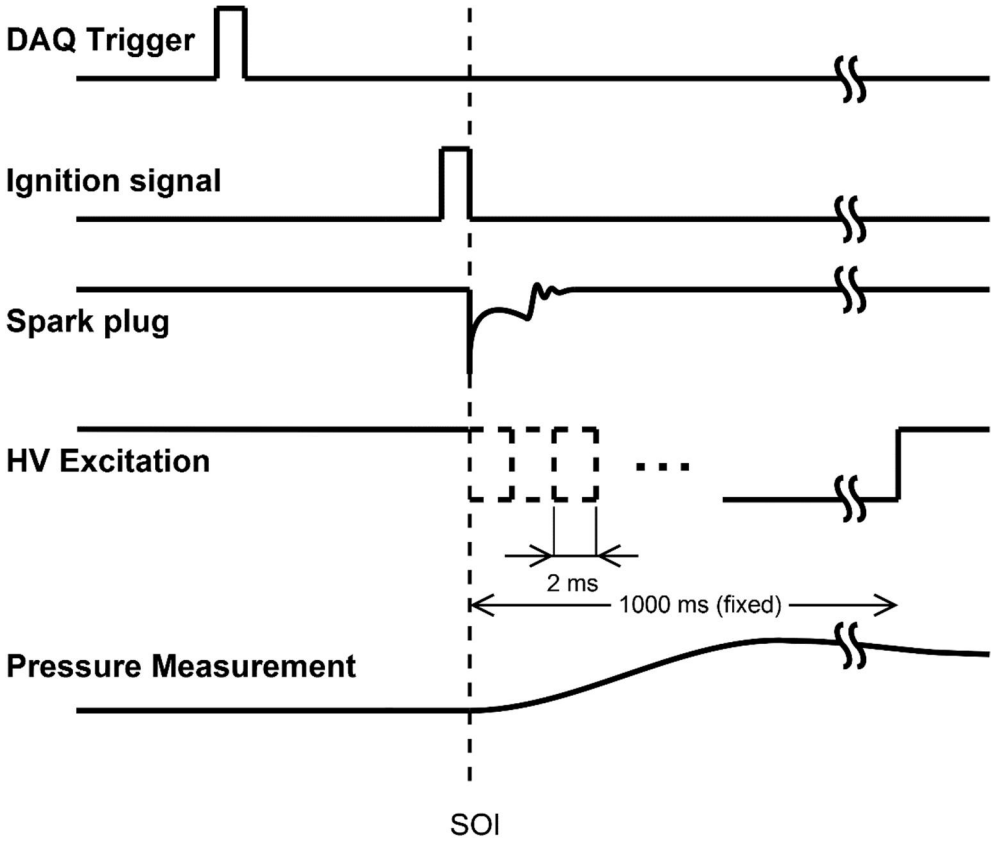

Figure 4.4 Timing chart of timing sweep experiment by varying t_s at V_e = -7 kV and t_e = 1000 ms.

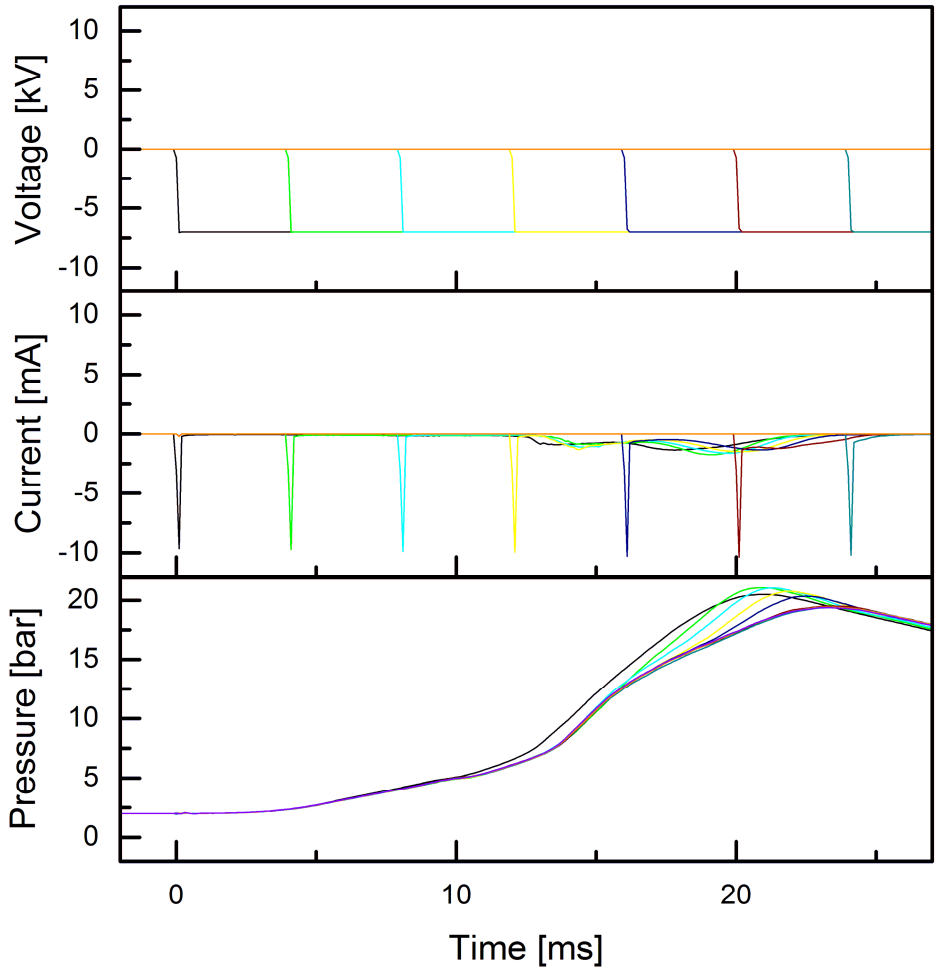

Figure 4.5 Voltage, current, and pressure versus time by varying t_s. V_e and t_e are set to -7 kV and 1000 ms, respectively.

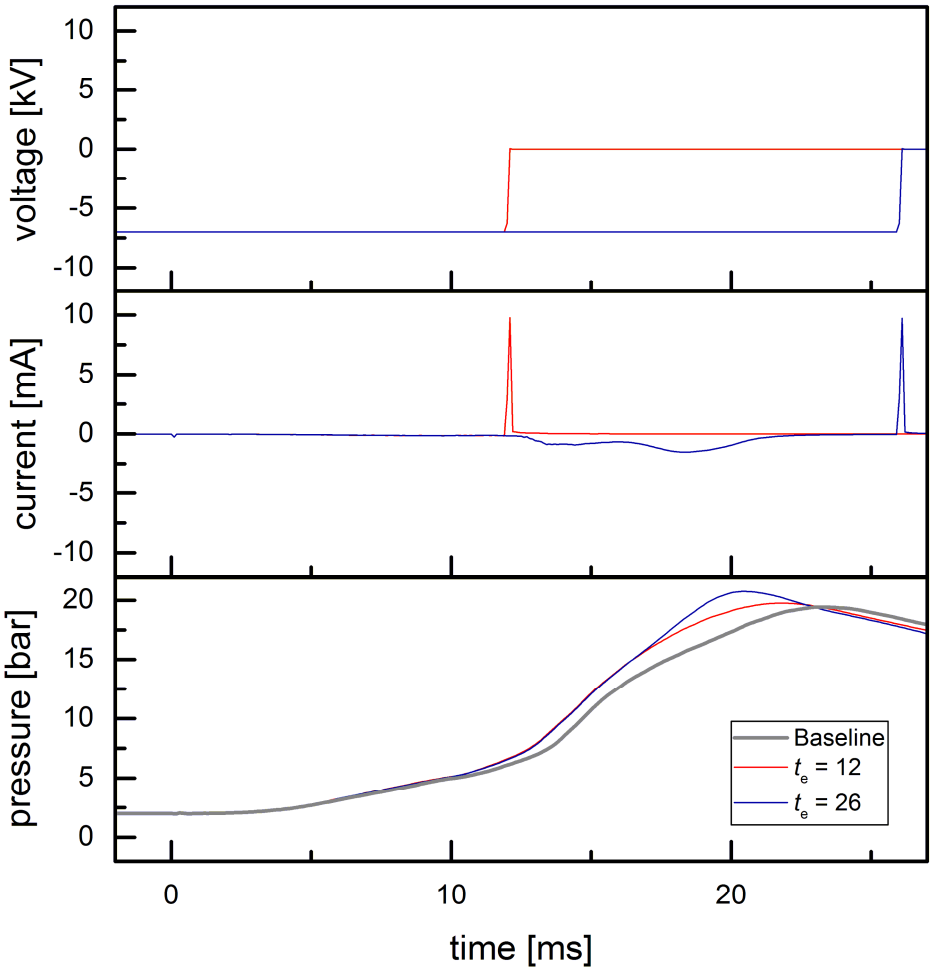

Figure 4.6 Comparison of representative samples when negative potential is applied to the electrode. V_e and t_s are set to -7 kV and -800 ms, respectively.

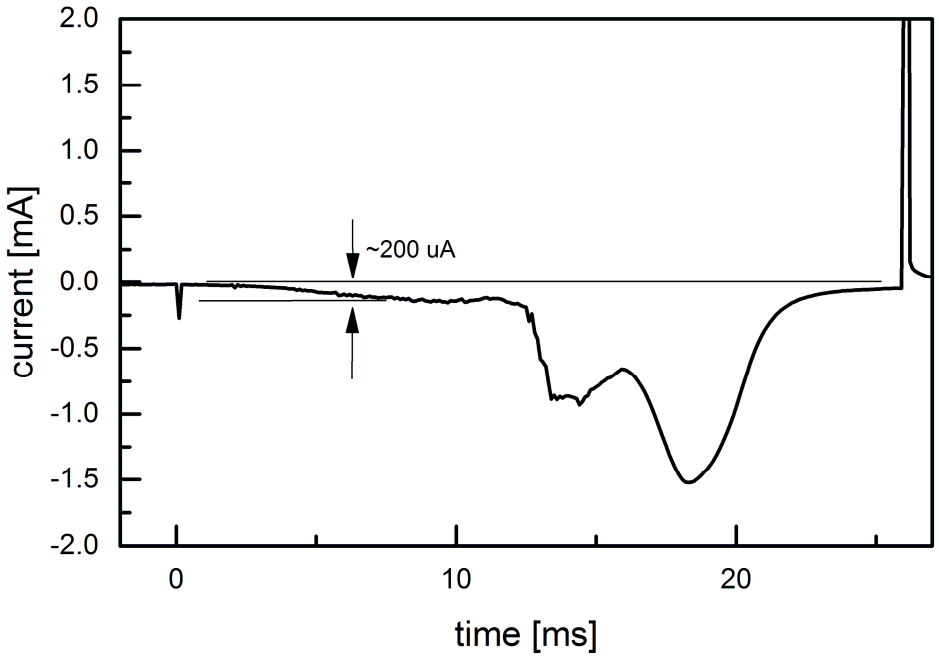

Figure 4.7 Magnified graph of current. V_e, t_s, and t_e are set to -7 kV, -800 ms, and 26 ms, respectively.

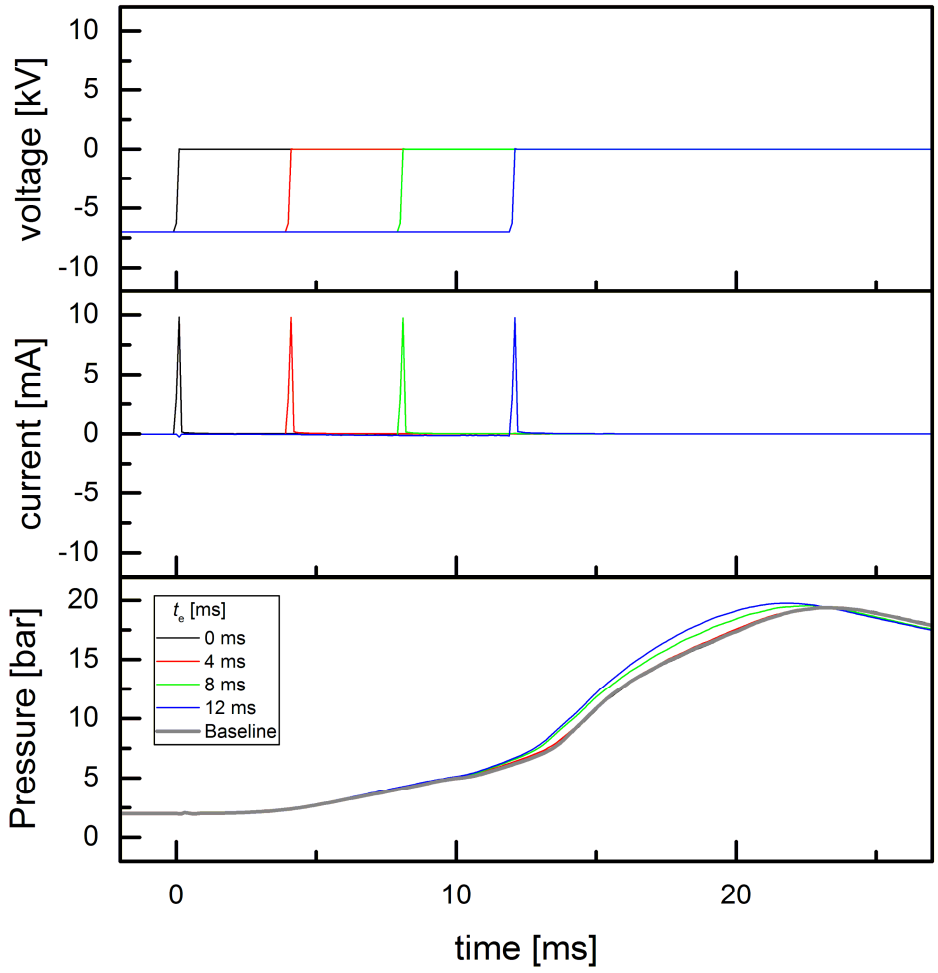

Figure 4.8 Voltage, current, and pressure versus time by varying t_e in sub-regime I of negative DC electric field.

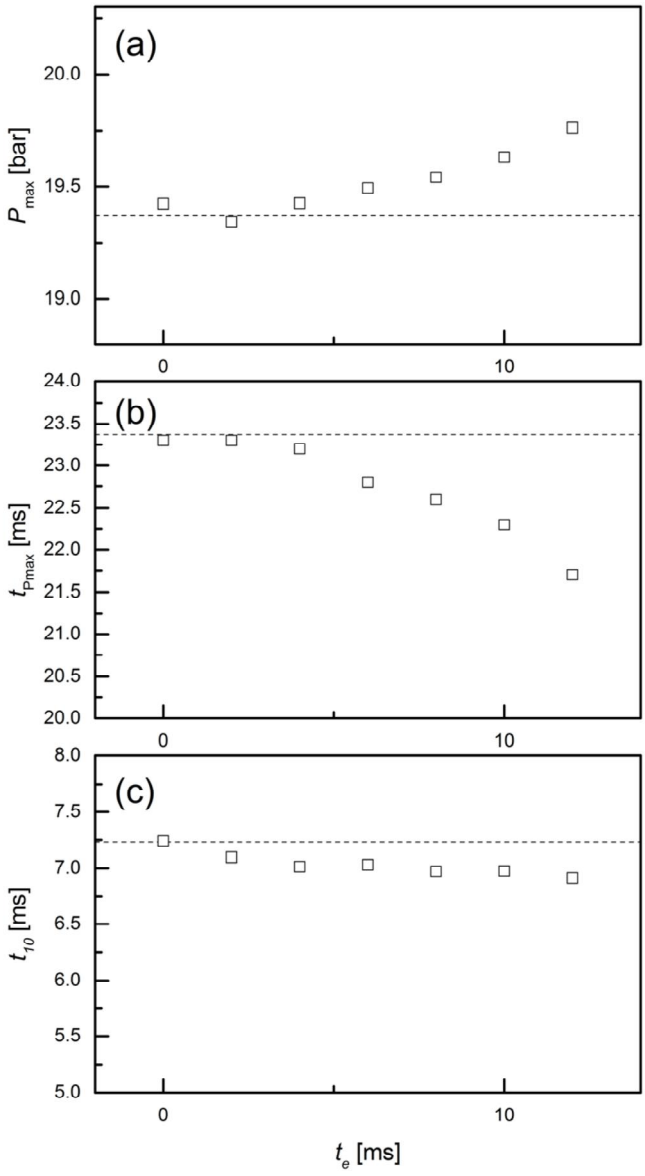

Figure 4.9 Flame propagation characteristics as a function of t_e in sub-regime I. (t_s = -800 ms). (a) P_{max}; (b) t_{Pmax}; (c) t_{10}

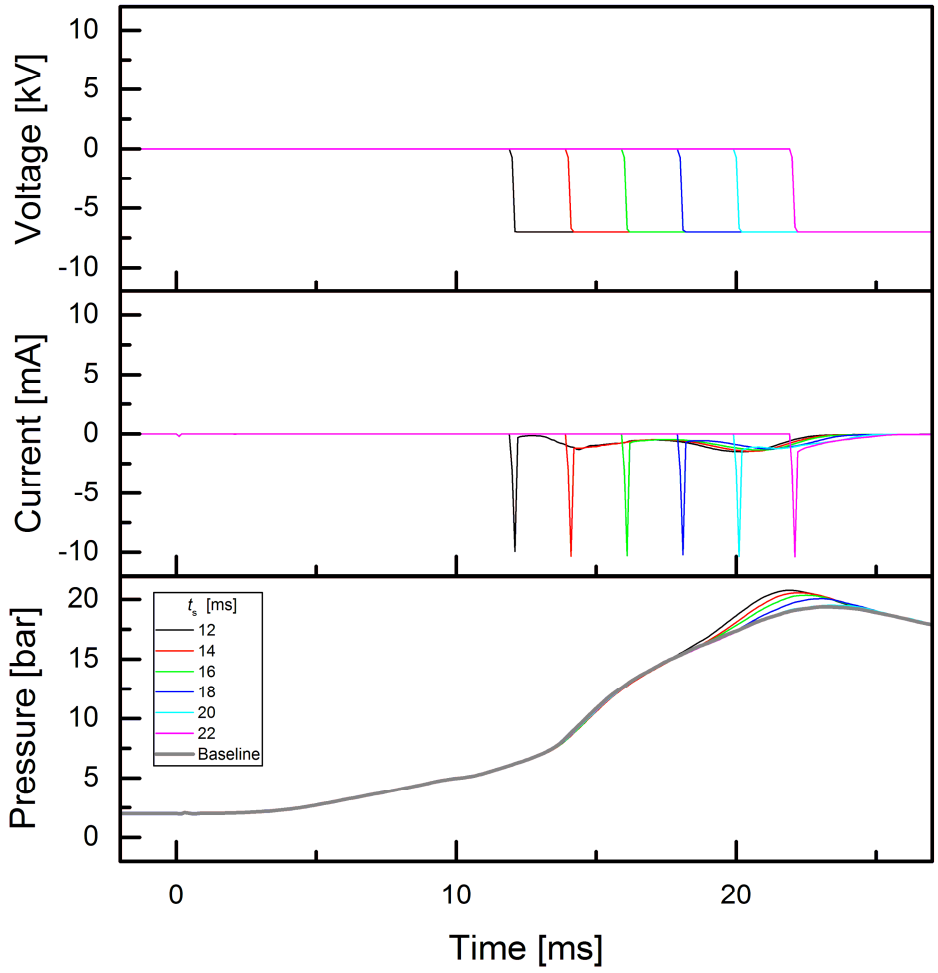

Figure 4.10 Voltage, current, and pressure versus time by varying start time in sub-regime II. (V_e = -7 kV and t_e = 1000 ms).

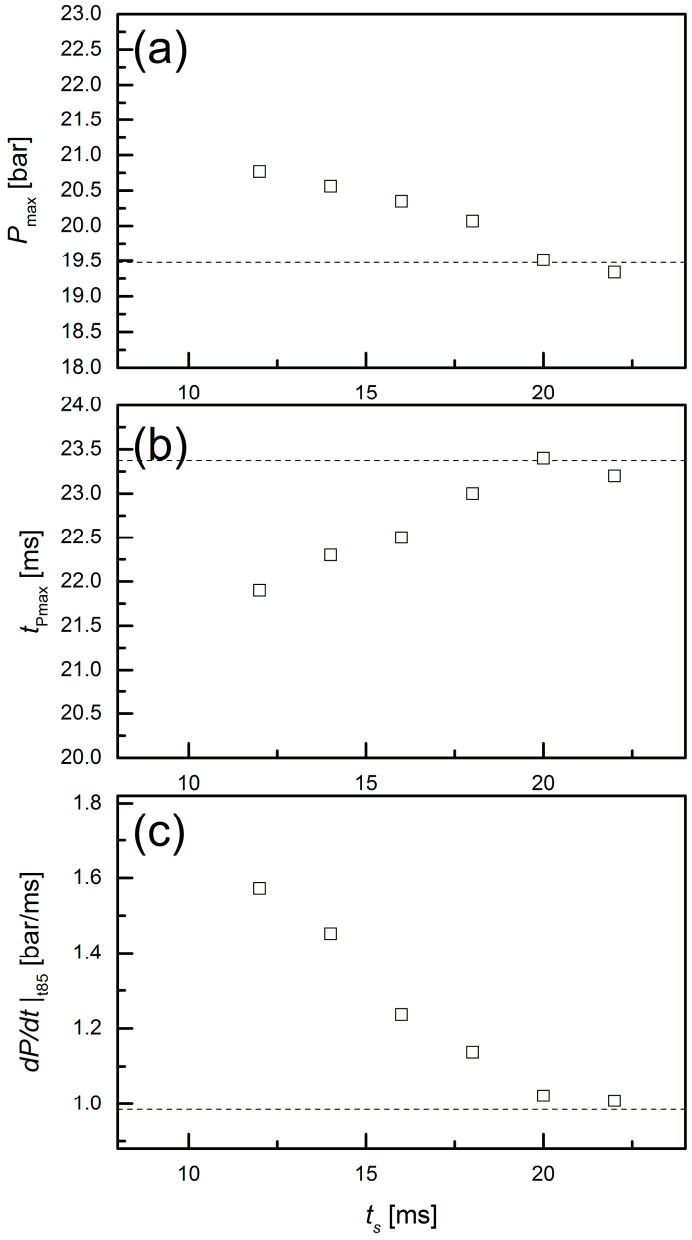

Figure 4.11 Flame propagation characteristics as a function of t_s in sub-regime II. (Ve = -7 kV and t_e = 1000 ms) (a) t_{Pmax}; (b) t_{10}; (c) $dP/dt|_{t85}$.

Chapter 5. Identification of Regimes

Three different effective regimes are classified based on the flame behavior and characteristics of the current flow (Figure 5.1). In this chapter, we will examine in more detail to elucidate the influence of electric field on flame propagation characteristics.

5.1 Regime I

Regime I is defined as an effective regime under the condition of positive potential—the electric field and the flame propagation are aligned in the opposite direction. As mentioned in Chapter 3, the positive electric field only has an effect within 2.5ms from SOI (i.e., $0 < x_b < 2\%$). However, once the enhancement of combustion arises, it is maintained even after disconnecting the high voltage—these improvements are observed near the 10% burn time. In this regime, the current flow of tens of μA was observed.

5.1.1 Effects of applied voltage

This section demonstrates the effects of DC excitation voltage when the duration is limited to regime I. Figure 5.2 shows the timing chart of the experiments. The start time and the end time of excitation are set to 0 and 4 ms, respectively. This duration is

long enough to saturate the affection of electric field in regime I. The excitation voltage was varied between -10 and 10 kV. Despite the variation of voltage, there is no transition from non-thermal to thermal plasma; this is because the distance between the flame front and the high voltage electrode is relatively far in this regime. The experiments are repeated nine times for each condition.

Figure 5.3 shows the results of representative samples, in which V_e is +10 kV and -10 kV, respectively. The current flow lower than 100 μA (in power) was observed in this regime, as specified in previous chapters. In both cases of the positive and the negative electric fields, the pressure graph shows the improvement in flame speed; however, the influence of negative potential is less efficient than that of the positive.

Figure 5.4 shows the combustion properties—including t_{pmax}, t_{10}, and dP/dt near the t_{10}—as functions of the excitation voltage. When the excitation voltage is relatively high, the influence of electric field shows a reasonably linear relationship; However, when the excitation voltage is relatively low, the influence of the electric field diminishes. The linear interpolation of data in the relatively high region is presented in Table 5.1. A threshold voltage, V_{th}, was determined as the cross point of the extrapolation of the linear fitting and the baseline (which is indicated by a horizontal dashed line in the figure). The slopes of the positive electric field are 1.31, 1.62, and 1.74 times steeper than those of the negative electric field, respectively. This result indicates that the polarity effect—influence of the positive electric field is more effective than that of the negative electric field—exists.

5.1.2 Effects of equivalence ratio

The Influence of equivalence ratio on the flame speed enhancement by applying the electric field in the regime I was investigated. The initial pressure and temperature are set as 2 bar and 85°C, respectively. The equivalence ratio varied between 0.85 and 1.15. The start time and end time of excitation are set as –100 and 4 ms, respectively. This duration is long enough to saturate the influence of electric field in regime I. The experiments are repeated at least10 times for each condition.

Figure 5.3 to 5.5 show the measured voltage, current, and pressure history by varying the equivalence ratio and the polarity of the excitation voltage. The results show a consistent increment of combustion characteristics by applying the electric field. The combustion characteristics including t_{pmax}, t_{10}, and dP/dt are listed in table 5.2. From this table, the normalized values of the characteristics including maximum pressure, 10% burn time, and pressure gradient near the 10% burn time are defined as the ratio of the value of the baseline condition (i.e., 0 kV is applied).

the enhancement of combustion characteristics with respect to the equivalence ratio are plotted in figure 5.6. Regardless of the equivalent ratio, influence of positive electric field is more effective than that of the negative electric field. These observations agree with the result of polarity effect, mentioned in Chapter 5.1.1. The enhancements are minimized in in stoichiometric condition; and greater enhancements were observed in the lean condition compared to those of rich or stoichiometric condition.

5.1.3 Influences of electrons

When the positive potential is applied to the high voltage electrode, the negatively charged particles—especially electrons—are attracted toward the unburned gas zone. Whereas the negative potential is applied to it, positive ions move toward the unburned gas zone [35]. In previous studies [8], [18], [36], positive particles play a bigger role than negative particles; therefore, previous papers pay attention to the results of negative DC electric field when the directions of the electric field and flame propagation are same. Specifically, Meng et al.[13] studied the only case of the negative potential in constant volume chamber.

However, regime I in this paper shows a contradictory phenomenon. Rather, this observation agrees with the result of HF excitation. Cha et al. [12] and Wolk et al. [23] applied 1 kHz and 2.45 GHz in a constant volume chamber, much higher than the boundary frequency of ionic wind [4], and reported accelerated flame kernel growth in the early stage of combustion. In high frequencies, the momentum of ions, which are heavy compared to the electrons, is neglected; in addition, the movement of free electrons is known to dominate the enhancement. Considering that the free electrons are attracted toward the preheat zone, it is reasonable to conclude that the movement of electrons influenced the flame propagation in regime I.

5.2 Regime II

Regime II, which is named sub-regime I in Chapter 4, is classified by the current flow when the negative potential is applied (i.e., when the electric field and flame propagation are aligned in the same direction). In regime II, there is a slight increment of the current as the flame propagates, and this current is saturated in approximately 200 μA at the point of 20% burned mass fraction. Furthermore, flame propagation speed increases linearly with the duration of applied electric field in this regime.

5.2.1 Ionic wind effect

In the previous research, the effects of DC electric field on flame propagation are elucidated as an ionic wind. When the DC electric field is applied to the flame, the charged particles are attracted toward the electrodes. Especially, the bulk motion, the positive ions including H_3O^+ and HCO^+ in the flame zone attracted to the negative electrode, is treated as a major term [18], [36]. Therefore, many previous studies pay attention to the case of negative potential (i.e., in which the directions of flame propagation and electric field are same, as shown in Figure 4.1). The results of this study in regime II are also explained by the ionic wind effect. Although the effect of the negative electric field per unit time in this regime is less efficient than that of the positive electric field in regime II, the total enhancement in regime II is better than that of regime I. This is because the effective duration in regime II is longer than that of regime I.

5.3 Regime III

Regime III appears promptly after regime II, as mentioned above. When the mass burn fraction is greater than 20%, a sharp increase in current flow up to ~1mA is detected. Furthermore, the dramatic rise in peak pressure and the advance of its timing are observed in the last period of combustion (x_b > 85%).

5.3.1 Current flow and electrical discharge

The experimental results of the positive and the negative potentials are compared in Figure 5.9. The excitation timing is fixed at t_s = 12 ms and t_e = 30 ms. Beyond the saturation point (boundary of regime II and III), the current graphs show sharp increment and peak values. Furthermore, this figure Figure 5.9 shows a diode-like behavior of current: The application of the negative potential causes an approximately 10-fold greater peak current flow compare to that of the positive one.

Tomcik et al. [37] investigated this diode-like behavior of flame and measured that the electrical resistance differs more by than one order of magnitude with respect to the direction of DC electric field. They assumed that the electron is the main charge carrier because the mean velocity of ions is slower than electrons. When the positive potential is applied to the burner, an “electron gap” occurs in the upper part of flame; therefore, the resistance of flame becomes higher than the opposite case. This polarity of resistance is consistent with the result of the present study. The distance between the flame front and the high voltage electrode is relatively short in

the last period of combustion, regime III. When the positive potential is applied to the electrode (Figure 5.10 (a)), the positive ions—of relatively low mean velocity–are shoved toward the burned gas zone, and travel to the burned gas zone, which is a relatively long distance. In the opposite case, as shown in Figure 5.10(b) the relatively fast electrons travel the long distance, and show relatively low electrical resistance.

The pressure history in Figure 5.9 shows the dramatic rise in the peak pressure and the advance of its timing near the last period of combustion. Two hypotheses are introduced to explain the result. First, the heat loss to the chamber wall is minimalized. As the flame speed increases, the duration of the interaction between the flame and the wall is shortened. Under the same initial condition, the net heat release inside the chamber does not largely change. However, the enhanced flame speed shortens the duration of contact between the flame and the wall of the constant volume chamber. Thus, the improved flame propagation minimizes the heat loss and increases the peak pressure. Second, the extra combustion of the unburned gas near the chamber wall is involved in the combustion. Rosocha et al. [38], [39] studied the effect of a dielectric barrier discharge in the premixed burner. They showed that the flame propagates downward (i.e., inside the tube of premix burner) in the cases of the high electrical excitation (>6W); the enhancement of propagation speed overcomes the quenching caused by the wall of the burner. In this manner, in the present study, it is reasonable that the mass burn fraction x_b is changed by the application of the electric field.

Assuming that the first hypothesis is the predominant mechanism, it cannot elucidate the change of pressure history occurs only within the last period of

combustion (t > 16 ms). That is, in the range of 12 < t < 16 ms of Figure 4.6, no distinguishable behavior of pressure between the red line (electric field is applied only in regime II) and the blue line (electric field is applied in both regimes II and III) can be observed. Furthermore, the increment of peak pressure is too large considering the advance of the timing of peak pressure. Therefore, it is reasonable that the second mechanism—extra combustion of unburned gas near the wall—is involved in the combustion process.

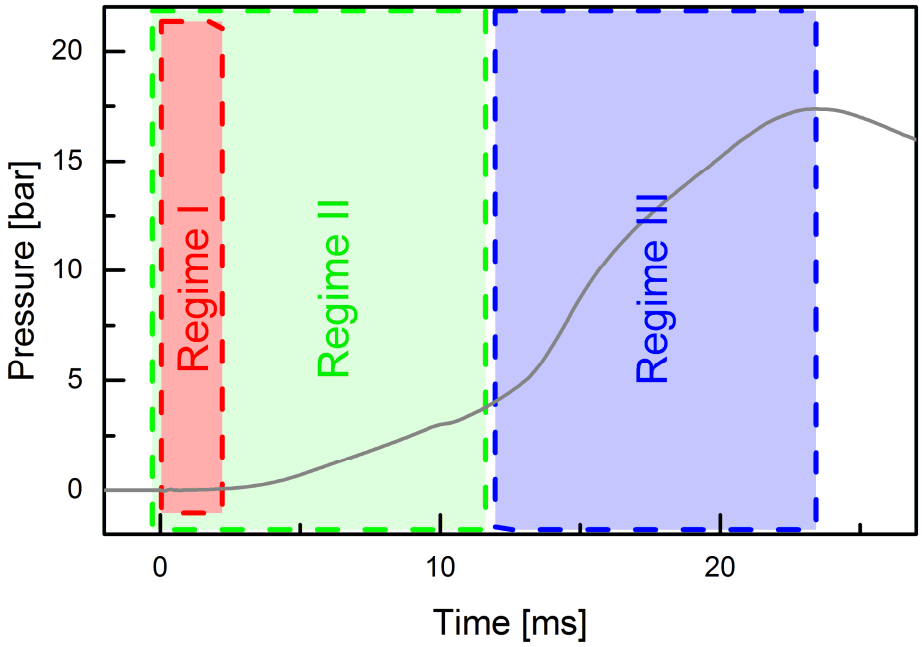

Figure 5.1 Classification of regimes with respect to high voltage excitation timing.

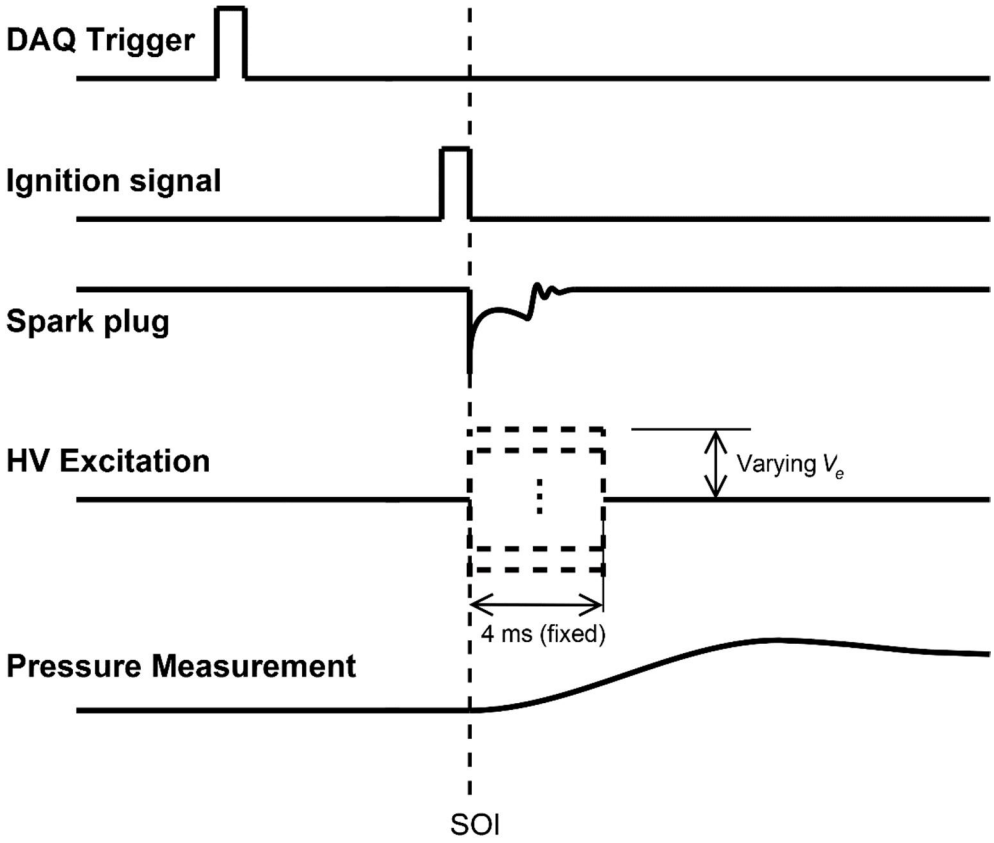

Figure 5.2 Timing chart of experiments for verify the influence of the excitation voltage, V_e, in regime I (t_s = 0 ms and t_e = 4 ms).

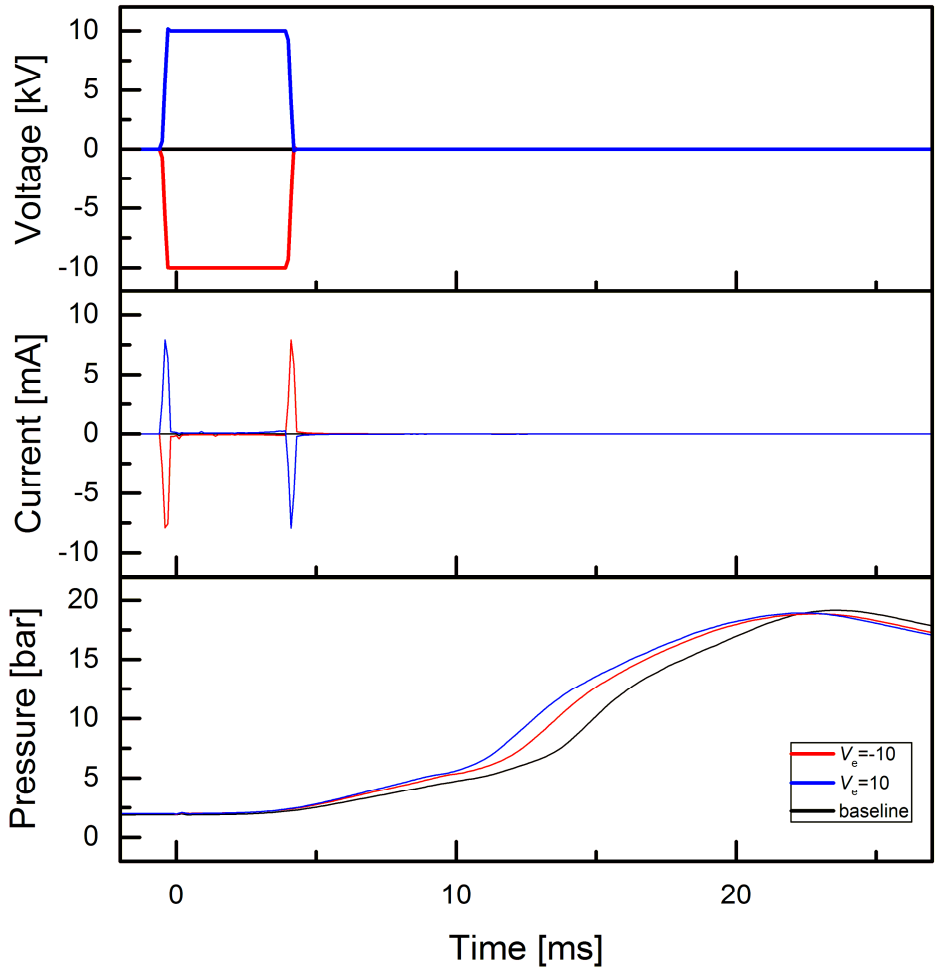

Figure 5.3 Voltage, current, and pressure versus time by varying V_e in regime I. (t_s = 0 and t_e = 4 ms).

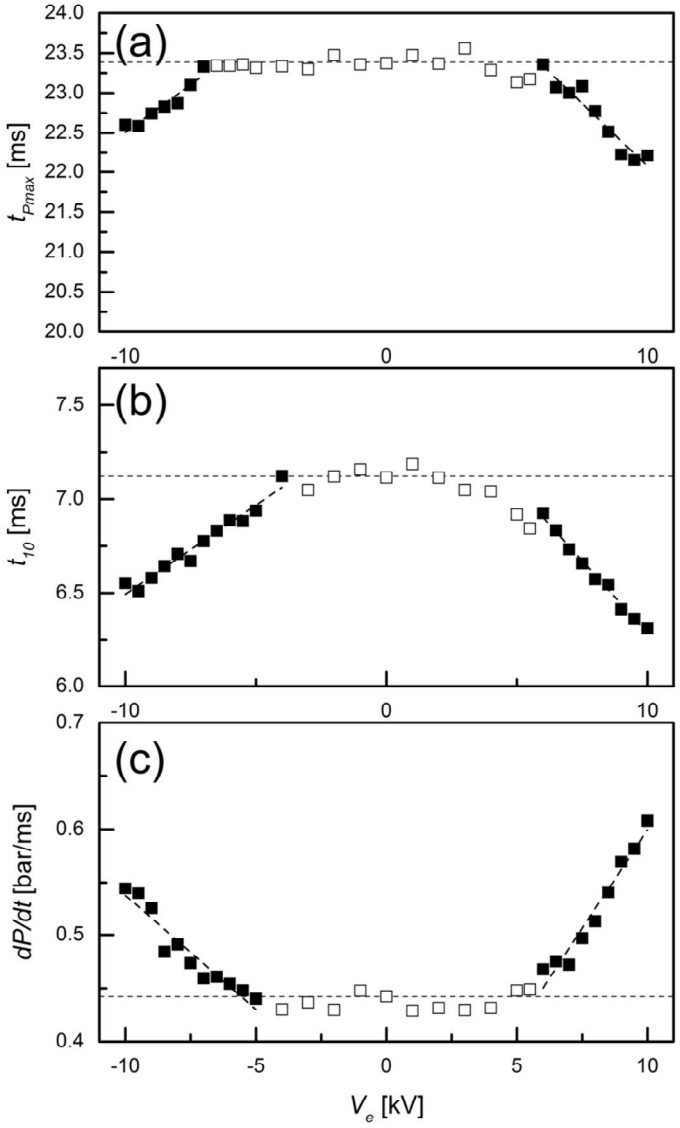

Figure 5.4 Influence of V_e on flame propagation characteristics (t_s = 0 ms and t_e = 4 ms). (a) t_{Pmax}; (b) t_{10}; (c) dP/dt.

Table 5.1 Result of linear fitting and threshold voltage.

Polarity	Property	Slope	Threshold voltage	R^2
Positive	t_{Pmax}	-0.3142	5.856	0.916
	t_{10}	-0.1537	4.585	0.988
	dP/dt	0.0373	5.787	0.951
Negative	t_{Pmax}	0.2388	-6.344	0.902
	t_{10}	0.0946	-3.388	0.954
	dP/dt	-0.0214	-5.572	0.903

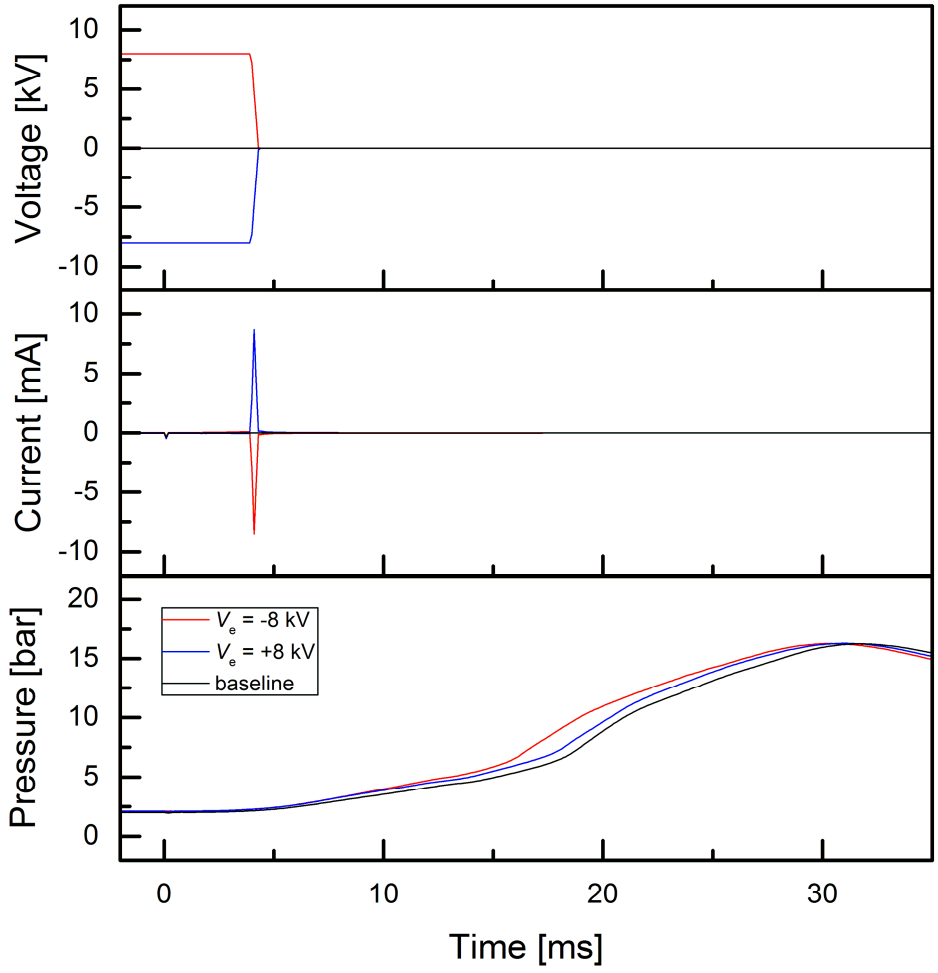

Figure 5.5 Voltage, current and pressure versus time with respect to the polarity of electric field in sub-regime I. (ϕ = 0.85)

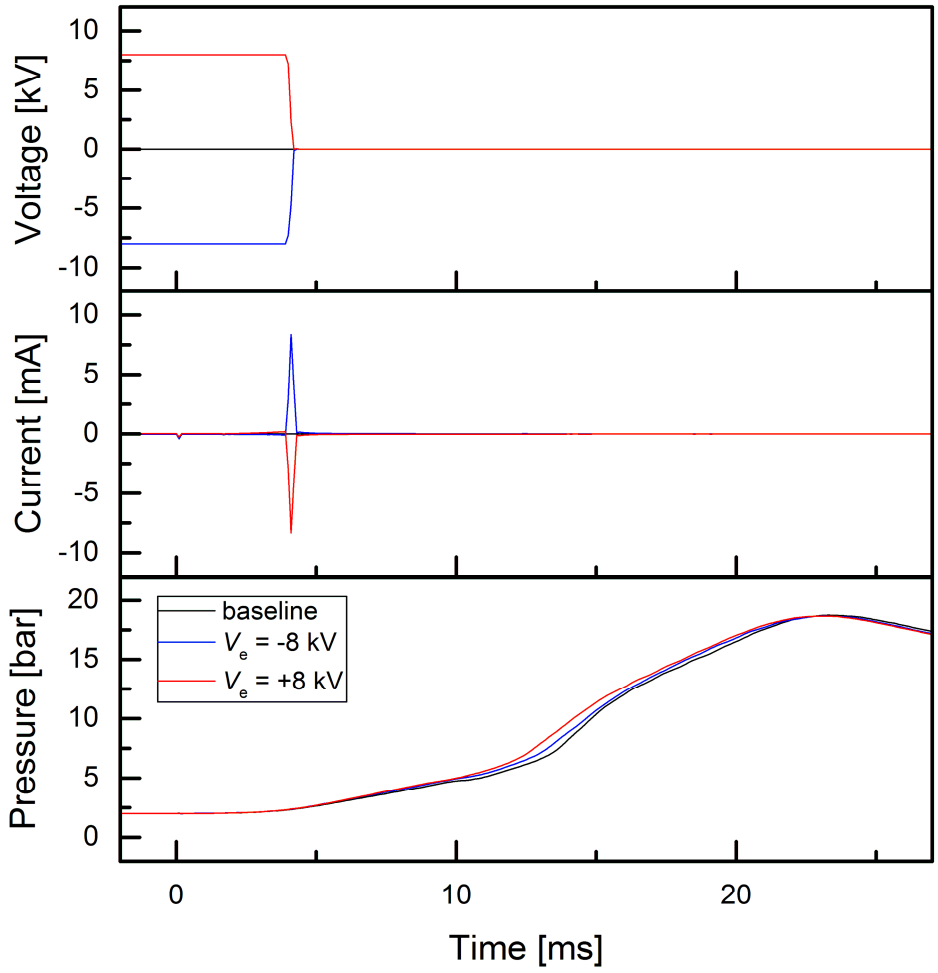

Figure 5.6 Voltage, current and pressure versus time with respect to the polarity of electric field in sub-regime I. (ϕ = 1.00)

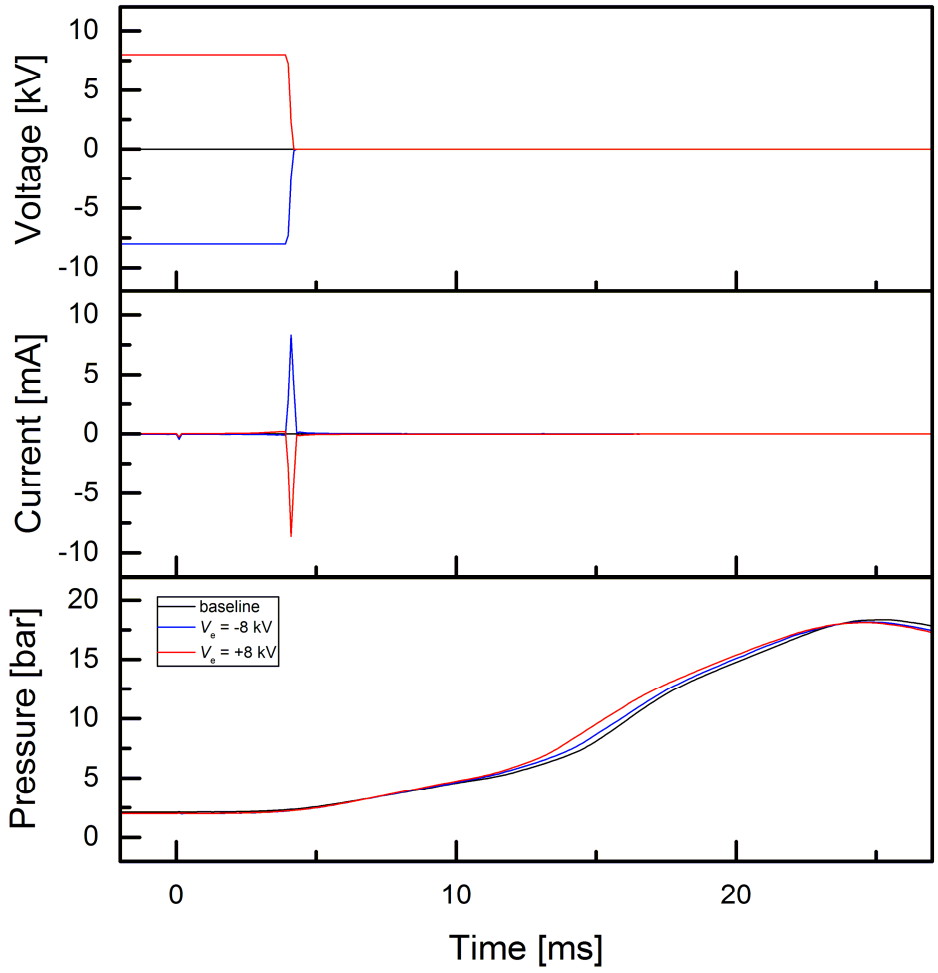

Figure 5.7 Voltage, current and pressure versus time with respect to the polarity of electric field in sub-regime I. (ϕ = 1.15)

Table 5.2 Combustion characteristics with respect to the equivalence ratio and the applied voltage.

Equivalence ratio	Applied Voltage [kV]	t_{pmax} [ms]	t_{10} [ms]	$dP/dt\|_{t10}$ [bar/ms]
0.85	-8	30.9	8.827	0.3083
	0	31.8	9.583	0.2754
	8	30.3	8.703	0.3528
1.00	-8	22.9	7.203	0.4549
	0	23.4	7.412	0.4232
	+8	23.0	7.204	0.4803
1.15	-8	24.5	7.664	0.4467
	0	25.3	8.038	0.4129
I	+8	24.6	7.587	0.4703

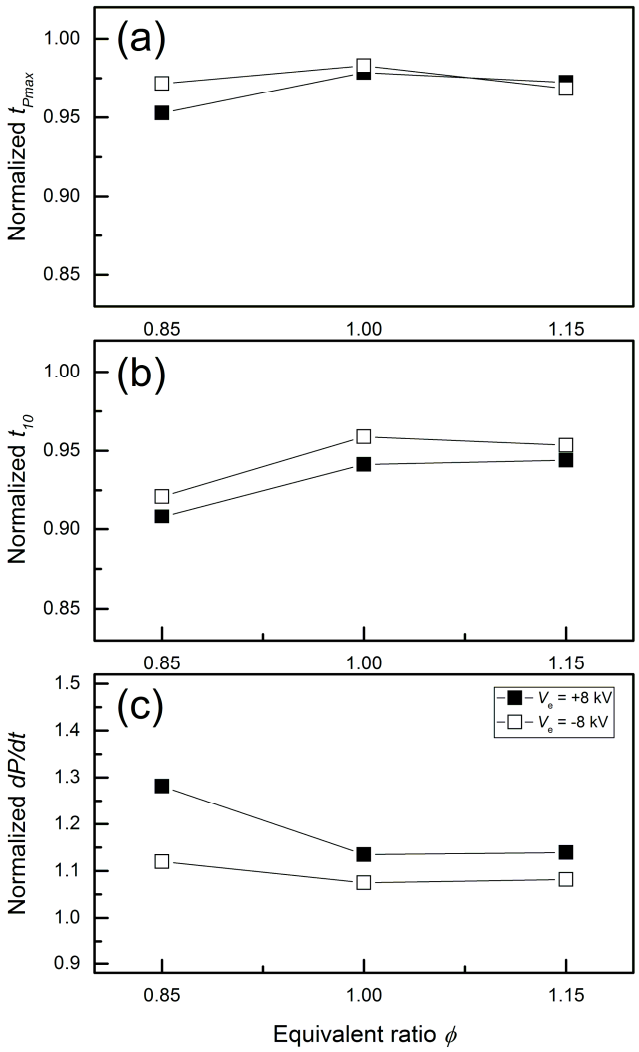

Figure 5.8 Normalized flame propagation characteristics as a function of ϕ in regime I. (a) P_{max} (b) t_{10} (c) $dP/dt|_{t10}$

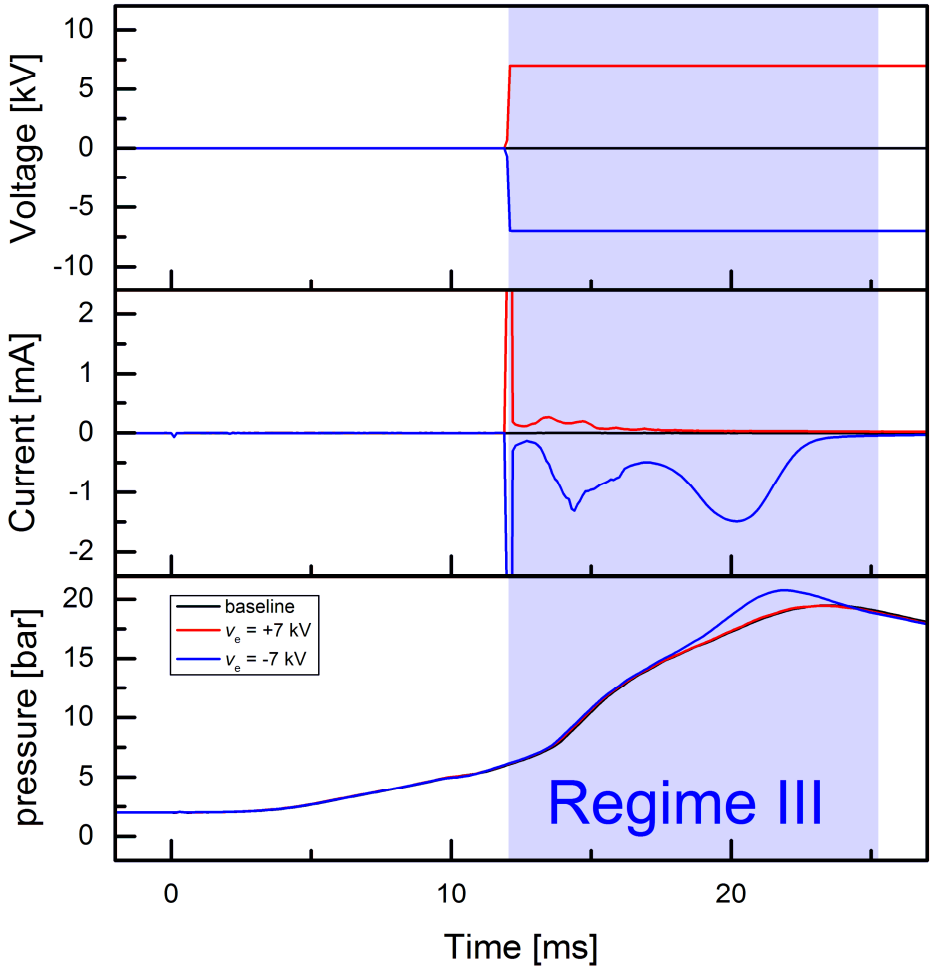

Figure 5.9 Voltage, current, and pressure versus time by varying V_e in regime III. (t_s = 12 and t_e = 30 ms).

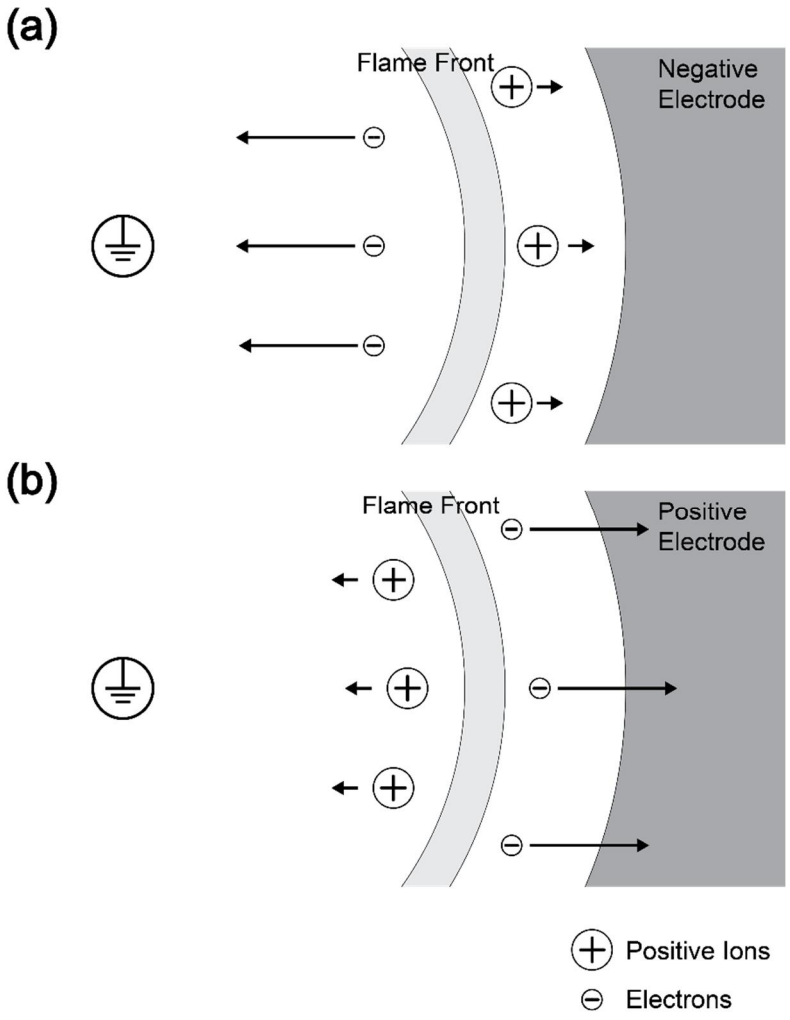

Figure 5.10 Polarity effect of resistance. (a) positive electric field (b) negative electric field.

Chapter 6. Concluding Remarks

In order to confirm the effects of DC electric field on the growth of flame, the flame propagation characteristics depending on the various timings of electric field excitation in a constant volume chamber were investigated via the present experiments. The cylindrical constant volume chamber in which the directions of the electric field and flame propagation are parallel to each other was designed to minimize the effects of shape factors. Moreover, the control and monitoring system was constructed to guarantee the repeatability of experiments.

By varying the polarity and timing of electric field excitation, we confirmed that the electric field before the start of ignition does not affect the flame propagation characteristics. Based on the characteristics of the current flow, three different effective regimes are classified.

Regime I is identified under the condition of the positive potential, which is when the directions of the electric field and the flame propagation are aligned in the opposite. The enhancement of combustion characteristics is observed only within the initial stage of the flame kernel growth. In this regime, flame characteristics linearly increase with respect to the extension of duration. The effect of negative excitation is also seen in this regime; however, it is less efficient than that of the positive. The effects of the polarity of excitation voltage and the equivalence ratio of the mixture are investigated in regime I. The effect of the electric field is more pronounced under the conditions of positive potential and lean mixture in this regime. The results cannot

be confirmed by the body force of positive ions, which is considered as a major mechanism of the enhancement by the DC electric field. Rather, it is elucidated that the free electrons attracted toward the preheat zone trigger the increment of reaction rate or thermodiffusive instability. The electrical power consumption in this region is measured as an order of 0.1 W.

Regime II is observed in the case of the negative voltage, which is when the electric field and the flame propagation are aligned in the same direction. The effectiveness per unit time in this regime is less than that of the positive voltage in regime I. Nonetheless, the total effect is better than that in regime I, for the effective duration is relatively long. The behavior of the flame characteristics in this regime corresponds with the conclusions of the ionic wind effect. The electrical power consumption is ~ 1 W in this regime.

Regime III is in which the drastic current flow is observed when a negative potential is applied to the electrode, because the flame front and the high voltage electrode become closer to each other at the end of combustion. A drastic increase in the peak pressure and the advance of its timing are observed near the last period of combustion. These results are explained as the extra combustion of unburned gas near the wall. The electrical power consumption in regime III is up to 10 W, tens of times higher than that in regime II.

In addition to the ionic wind effect which is considered as a major mechanism of the DC electric field, the results of the experiments confirm that the chemical reaction rate and the extra combustion of unburned gas near the wall are able to play an important role. The aims of this dissertation are not to investigate the continuous

flame (e.g., Bunsen burner), but to investigate the transient flame in the constant volume chamber. The results presented in this dissertation show a possibility of the electric field excitation for application of the reciprocating engines. Considering that the experimental condition of this study is fixed in premixed air-fuel mixture, it is likely to applicable to engines with low viscosity fuels such as CNG. Further studies will be required to applying the electric field assisted combustion systems to the real engines in the future.

Bibliography

[1] A. Starikovskiy and N. Aleksandrov, "Plasma-assisted ignition and combustion," *Prog. Energy Combust. Sci.*, vol. 39, no. 1, pp. 61–110, Feb. 2013.

[2] T. Ombrello, S. H. Won, Y. Ju, and S. Williams, "Flame propagation enhancement by plasma excitation of oxygen. Part I: Effects of O3," *Combust. Flame*, vol. 157, no. 10, pp. 1906–1915, 2010.

[3] W. T. Brande, "The Bakerian lecture: On some new electro-chemical phenomena," *Philos. Trans. R. Soc.*, vol. 104, no. January, pp. 51–61, Jan. 1814.

[4] H. C. Jaggers and A. von Engel, "The effect of electric fields on the burning velocity of various flames," *Combust. Flame*, vol. 16, no. 3, pp. 275–285, 1971.

[5] H. F. Calcote and R. N. Pease, "Electrical Properties of flames," *Ind. Eng. Chem.*, vol. 43, p. 2726, 1951.

[6] M. K. Kim, S. H. Chung, and H. H. Kim, "Effect of AC electric fields on the stabilization of premixed bunsen flames," *Proc. Combust. Inst.*, vol. 33, no. 1, pp. 1137–1144, 2011.

[7] M. K. Kim, S. H. Chung, and H. H. Kim, "Effect of electric fields on the stabilization of premixed laminar bunsen flames at low AC frequency: Bi-ionic wind effect," *Combust. Flame*, vol. 159, no. 3, pp. 1151–1159, Mar. 2012.

[8] J. Kuhl, G. Jovicic, L. Zigan, and A. Leipertz, "Transient electric field response of laminar premixed flames," *Proc. Combust. Inst.*, vol. 34, no. 2, pp. 3303–3310, Jan. 2013.

[9] M. Kono, F. B. Carleton, A. R. Jones, and F. J. Weinberg, "The effect of nonsteady electric fields on sooting flames," *Combust. Flame*, vol. 78, no. 3–4, pp. 357–364, 1989.

[10] J. W. Rinker and W. Virginia, "Electrical Impedance of Methane Flat Flame Abstract Electrical Impedance of Methane Flat Flame," 2002.

[11] M. K. Kim, S. K. Ryu, S. H. Won, and S. H. Chung, "Electric fields effect on liftoff and blowoff of nonpremixed laminar jet flames in a coflow," *Combust. Flame*, vol. 157, no. 1, pp. 17–24, 2010.

[12] M. S. Cha and Y. Lee, "Premixed Combustion Under Electric Field in a Constant Volume Chamber," *IEEE Trans. Plasma Sci.*, vol. 40, no. 12, pp. 3131–3138, Dec. 2012.

[13] X. Meng, X. Wu, C. Kang, A. Tang, and Z. Gao, "Effects of Direct-Current (DC) Electric Fields on Flame Propagation and Combustion Characteristics of Premixed CH 4 /O 2 /N 2 Flames," *Energy & Fuels*, no. Dc, pp. 6612–6620, Oct. 2012.

[14] H. Duan, X. Wu, T. Sun, B. Liu, J. Fang, C. Li, and Z. Gao, “Effects of electric field intensity and distribution on flame propagation speed of CH4/O2/N2 flames,” *Fuel*, vol. 158, pp. 807–815, 2015.

[15] M. Cha, S. Lee, K. Kim, and S. Chung, “Soot suppression by nonthermal plasma in coflow jet diffusion flames using a dielectric barrier discharge,” *Combust. Flame*, vol. 141, no. 4, pp. 438–447, Jun. 2005.

[16] S. Lee and C. Park, “Effect of electric fields on the liftoff of nonpremixed turbulent jet flames,” *Plasma Sci. IEEE ...*, vol. 33, no. 5, pp. 1703–1709, Oct. 2005.

[17] J. D. B. J. van den Boom, A. Konnov, A. M. H. H. Verhasselt, V. N. Kornilov, L. P. H. de Goey, and H. Nijmeijer, “The effect of a DC electric field on the laminar burning velocity of premixed methane/air flames,” *Proc. Combust. Inst.*, vol. 32, no. 1, pp. 1237–1244, 2009.

[18] D. Wisman, S. Marcum, and B. Ganguly, “Electrical control of the thermodiffusive instability in premixed propane–air flames,” *Combust. Flame*, vol. 151, no. 4, pp. 639–648, Dec. 2007.

[19] Y. Xiong, M. S. Cha, and S. H. Chung, “AC electric field induced vortex in laminar coflow diffusion flames,” *Proc. Combust. Inst.*, vol. 35, no. 3, pp. 3513–3520, 2015.

[20] B. Lewis, “The effect of an electric field on flames and their propagation,” *J. Am. Chem. Soc.*, vol. 53, no. 4, pp. 1304–1313, 1931.

[21] S. Marcum and B. Ganguly, “Electric-field-induced flame speed modification,” *Combust. Flame*, vol. 143, no. 1–2, pp. 27–36, Oct. 2005.

[22] S. H. Won, M. S. Cha, C. S. Park, and S. H. Chung, “Effect of electric fields on reattachment and propagation speed of tribrachial flames in laminar coflow jets,” vol. 31, pp. 963–970, 2007.

[23] B. Wolk, A. DeFilippo, J.-Y. Chen, R. Dibble, A. Nishiyama, and Y. Ikeda, “Enhancement of flame development by microwave-assisted spark ignition in constant volume combustion chamber,” *Combust. Flame*, vol. 160, no. 7, pp. 1225–1234, Jul. 2013.

[24] M. Saito, M. Sato, and K. Sawada, “Variation of flame shape and soot emission by applying electric field,” *J. Electrostat.*, vol. 39, no. 4, pp. 305–311, Aug. 1997.

[25] A. P. Chattock, “On the Velocity and Mass of the Ions in the Electric Wind in Air,” *Philos. Mag.*, vol. 48, no. 294, pp. 401–421, 1899.

[26] D. B. Go, R. A. Maturana, T. S. Fisher, and S. V. Garimella, “Enhancement of external forced convection by ionic wind,” *Int. J. Heat Mass Transf.*, vol. 51, no. 25–26, pp. 6047–6053, 2008.

[27] S. H. Won, S. K. Ryu, M. K. Kim, M. S. Cha, and S. H. Chung, “Effect of electric fields on the propagation speed of tribrachial flames in coflow jets,” *Combust. Flame*,

vol. 152, no. 4, pp. 496–506, 2008.

[28] R. J. Bowser and F. J. Weinberg, “Electrons and the emission of soot from flames,” *Nature*, vol. 249, no. 5455, pp. 339–341, 1974.

[29] A. ATA, J. S. COWART, A. VRANOS, and B. M. CETEGEN, “Effects of Direct Current Electric Field on the Blowoff Charactericsitcs of Bluff-body Stabilized Conical Premixed Flames,” *Combust. Sci. Technol.*, vol. 177, no. 7, pp. 1291–1304, Jul. 2005.

[30] J. B. Heywood, *Internal Combustion Engine Fundamentals*. McGraw-Hill, 1988.

[31] Z. Huang, Q. Wang, H. Miao, X. Wang, K. Zeng, B. Liu, and D. Jiang, “Study on dimethyl ether - Air premixed mixture combustion with a constant volume vessel,” *Energy and Fuels*, vol. 21, no. 4, pp. 2013–2017, 2007.

[32] G. A. Lavoie, J. B. Heywood, and J. C. Keck, “Experimental and Theoretical Study of Nitric Oxide Formation in Internal Combustion Engines,” *Combust. Sci. Technol.*, vol. 1, no. 4, pp. 313–326, 1970.

[33] T. O. and Y. Ju†, P. Princeton University New Jersey 08544, and, A. Fridman‡, and P. Drexel University Pennsylvania 19104, “Kinetic Ignition Enhancement of Diffusion Flamesby Nonequilibrium Magnetic Gliding Arc Plasma,” *Aiaa J.*, vol. 46, no. 10, pp. 2424–2433, 2008.

[34] L. A. Rosocha, Y. Kim, G. K. Anderson, J. O. Lee, and S. Abbate, “Decomposition of Ethane in Atmospheric-Pressure Dielectric-Barrier Discharges: Experiments,” *IEEE Trans. Plasma Sci.*, vol. 34, no. 6, pp. 2526–2531, Dec. 2006.

[35] F. Altendorfner, J. Kuhl, L. Zigan, and A. Leipertz, “Study of the influence of electric fields on flames using planar {LIF} and {PIV} techniques,” *Proc. Combust. Inst.*, vol. 33, no. 2, pp. 3195–3201, 2011.

[36] J. M. Goodings, J. Guo, A. N. Hayhurst, and S. G. Taylor, “Current--voltage characteristics in a flame plasma: analysis for positive and negative ions, with applications,” *Int. J. Mass Spectrom.*, vol. 206, no. 1, pp. 137–151, 2001.

[37] P. Tomcik, P. Klaus, J. Kulhanek, and R. Trojan, “Influence of Electric Field on Stabilization of Flame From Poor Methane–Oxygen Mixture,” *IEEE Trans. Plasma Sci.*, vol. 41, no. 8, pp. 2230–2236, Aug. 2013.

[38] L. A. Rosocha, Y. Kim, G. K. Anderson, S. Abbate, and A. C. Framework, “Combustion Enhancement Using Silent Electrical Discharges,” no. June 2006, pp. 8–13, 2007.

[39] S. Stange, Y. Kim, V. Ferreri, L. A. Rosocha, and D. M. Coates, “Flame images indicating combustion enhancement by dielectric barrier discharges,” *IEEE Trans. Plasma Sci.*, vol. 33, no. 2 I, pp. 316–317, 2005.

요약(국문초록)

현대 인류가 소모하는 에너지의 80% 이상은 화석연료의 연소과정으로부터 생산되고 있다. 이러한 점에서 보다 효율적이고 깨끗한 연소장치의 개발은 중요한 연구과제로 남아있다. 최근에는 연소장치에 고전압을 인가하여 화염 연소 특성을 개선하려는 신기술들이 연구되고 있다. 이는 비교적 적은 에너지의 소모로 연소 특성을 바꿀 수 있고, 반도체 및 제어기술의 발달에 따라 고전압 제어가 쉬워졌기 때문이다. 그러나 기존의 많은 연구에도 불구하고 전기장 인가로 인한 연소특성의 변화 메커니즘에 대해서는 아직 제한적인 설명만이 가능한 상황이다. 특히 화염이 발달하는 과정 중에 전기장 인가 타이밍이 미치는 영향에 대한 연구는 아직까지 미진한 상태이다.

본 연구의 목표는 전기장 인가 타이밍이 정적 연소실 내 화염전파 특성에 미치는 영향을 조사하는 것이다. 이를 위하여 본 논문에서는 실린더의 벽면을 고전압 전극으로 활용함으로써 화염 연소 방향과 전기장 인가 방향이 평행한 정적 연소실을 제안하였다. 또한 각 실험간 오차를 줄이기 위해 전기장 인가 시간과 점화시간, 실험결과 측정을 동기화 하고 자동으로 실험을 수행할 수 있는 시스템을 개발하였다.

전기장 인가 극성과 인가 타이밍의 변화에 따른 화염의 거동 및 전류를 관찰한 결과, 그 경향에 따라 다음과 같이 크게 3가지 영역으로 구분

할 수 있었다. Regime I은 양전압을 인가했을 때의 효과가 나타나는 영역이다. 이 영역은 화염핵이 발달하기 시작하는 연소 초기에만 나타나며, 이외의 구간에서는 양전압으로 인한 연소속도 증진효과가 관찰되지 않는다. 이 영역의 연소속도 증진효과는 자유전자에 의한 화학반응속도 변화로 설명이 가능하였다. Regime I 에서 인가 전압의 극성 및 당량비의 변화에 따른 연소 특성의 변화를 관찰하였다. 양전압을 인가하였을 때 및 당량비가 낮은 경우에 연소속도 증진 효과가 더 크게 나타나는 것을 확인하였다. Regime II와 Regime III는 음전압을 인가했을 때의 효과가 나타나는 영역으로, 전류의 흐름에 따라 구분이 가능하다. Regime II는 연소개시로부터 20% burn time 이내에서 관찰 되었다. 전류가 포화되는 현상을 보이는 구간이다. 이 영역의 음전압 인가 효과는 Regime I의 양전압 인가 효과와 비교하였을 때, 단위 시간당 증진효과는 더 떨어진다. 그러나 Regime I 보다 더 긴 시간에 걸쳐 화염 연소특성에 영향을 미칠 수 있기 때문에 최종적인 연소속도 증진효과는 regime I에 비해 더 크게 나타난다. Regime III는 Regime II 직후 급격한 전류증가가 관찰되는 영역이다. 이 구간에 인가된 음전압으로 인한 연소속도 증진 효과는 연소 말기의 압력곡선을 급격하게 변화시킨다. 이 현상은 벽면 주변에 존재하는 미연가스가 추가적으로 연소하면서 생기는 것으로 설명 할 수 있다.

본 연구에서는 기존의 DC 전기장 인가로 인한 연소 특성 증진의 주요 원인으로 거론되었던 이온풍 효과 외에도 자유전자의 여기에 의한 화학

반응속도 증가 메커니즘이나 벽 주변에서 미연가스의 추가적인 연소현상 또한 지배적인 메커니즘으로 동작 할 수 있음을 확인하였다. 본 연구의 결과를 통하여 전기장 인가장치가 CNG 엔진과 같은 왕복운동 엔진의 성능향상에 응용 될 수 있는 가능성을 제시하였다. 추후 추가적인 연구를 통하여 실제 엔진의 성능향상 연구에 기여 할 수 있을 것으로 기대된다.

주요어 : 전기장, 연소속도, 이온풍, 예혼합 화염, 정적연소실

학 번 : 2006-20938